Geophys. J. Int. (2006) **167,** 24–42 doi: 10.1111/j.1365-246X.2006.03087.x

Palaeomagnetism of Palaeozoic ultrabasic rocks from the Sudetes Mts (SW Poland): tectonic implications

M. Kądziałko-Hofmokl,[1] M. Jeleńska,[1] P. Bylina,[2] E. Dubińska,[3] K. Delura[3] and K. Nejbert[3]

[1] *Institute of Geophysics, Polish Academy of Sciences, ul. Ks. Janusza* 64, 01-452 *Warsaw, Poland. E-mail: magdahof@igf.edu.pl*
[2] *Institute of Geological Sciences, Polish Academy of Sciences, Warsaw, ul.Twarda* 51/55, 00-818 *Warszawa, Poland*
[3] *Faculty of Geology, Warsaw University, ul. Żwirki i Wigury* 93, 02-089 *Warszawa, Poland*

Accepted 2006 May 31. Received 2006 May 4; in original form 2005 May 25

SUMMARY

A complex palaeomagnetic, rock-magnetic and mineralogical study of ultrabasic rocks from the Sowie Góry Block (GSB) and Jordanów–Gogołów Serpentinite Massif (JGSM) revealed the presence of several components of natural remanent magnetization (NRM). The authors found three groups of Palaeozoic as well as Triassic and Recent components of the geomagnetic field. The Palaeozoic components of NRM are carried mainly by magnetite of several generations formed during several serpentinization episodes. Permo-Carboniferous component (A1) present overall the Sudetes was isolated in one JGSM and two GSB exposures, whereas the Late Devonian–Early Carboniferous component (A2) was found in two exposures from the GSB. The corresponding remanent components were already revealed in palaeontologically dated sediments from other West Sudetic units. In the GSB, it was probably acquired during its unroofing dated isotopically for *ca.* 370–360 Ma. The newly determined group of Palaeozoic directions (A3) was found in three localities from JGSM and in two from GSB is interpreted as the oldest overprint. In JGSM, it was acquired probably shortly after the first oceanic serpentinization phase dated isotopically for *ca.* 400 Ma. Its acquisition in GSB corresponds to the time of emplacement of ultrabasic xenoliths dated isotopically at *ca.* 390 Ma. So we suppose that the mean A3 calculated for five exposures corresponds to the 380–400 Ma time span and that at that period both massifs formed one microplate. Mean inclination of A3 places this microplate at 380–400 Ma at the palaeolatitude of 23°S, whereas the West Sudetes were situated during the Early Devonian at 16°S. We suggest that during the Early Devonian the microplate comprising GSB and JGSM massifs was situated to the south from the West Sudetes and accreted them during Middle–Late Devonian.

Key words: ophiolite, palaeomagnetism, Palaeozoic, rock magnetism, Sudetes.

1 INTRODUCTION

The main goal of a palaeomagnetic study of the West Sudetic rocks undertaken about 15 years ago was to reveal the geotectonic history of the Sudetes Mts and their position relaive to the Baltica plate during formation of the European Variscan Belt. The West Sudetes lie to the northeast of the Elbe Fault Zone, at the eastern part of the Saxo-Thurigian Zone and the northeastern part of the Bohemian Massif. The metamorphic Niemcza Shear Zone separates them from the Eastern Sudetes. The Saxothuringian Zone and the Bohemian Massif belong to the Armorican Terrane Assemblage (ATA, Tait 1999)—the complex collage of Gondwana—derived terranes: Bohemian Massif, Saxo-Thuringian, Armorican Massif and Catalan Massif. According to Tait *et al.* (2000), palaeomagnetic data indicate that the ATA elements had drifted away from Gondwana during the Late Ordovician. During the Late Silurian–Early Devonian times, they were situated in proximity of the southern margin of Baltica, in palaeolatitudes of 20°–30°S. Final suturing and consolidation of ATA as well as rotation of the Bohemian Massif to its present orientation and closure of the Saxo-Thuringian basin had occurred by Late Devonian times (or Early Carboniferous, according to Winchester *et al.* 2002).

The West Sudetes form a mosaic composed of numerous of blocks of various origin, age and lithology. Palaeomagnetic investigations performed so far for many of them, yielded a sufficient number of results (see references in Jeleńska *et al.* 2003) that it was possible to construct of the Devonian—Permian fragment of the Western Sudetic Apparent Polar Wander Path (APWP) (Jeleńska *et al.* 2003). The Sudetic path fits the Baltica Apparent Polar Wander Path (Torsvik & Smethurst 1994) during the Devonian and Carboniferous times. During the Permo-Carboniferous, it shifts slightly to the East and returns to the Baltica one during the Middle Permian. Jeleńska *et al.*

(2003) ascribed this minor shift to formation and closure of a small basin.

This paper concerns two units that were not yet investigated palaeomagnetically: the Góry Sowie Block (GSB) and the Jordanów–Gogołów Serpentinite Massif (JGSM). Our aim is to contribute to the Sudetic database with new data from ultrabasic rocks exposed in the units of GSB and JGSM. In the course of our study, we will correlate the results of palaeomagnetic and mineralogical investigations with the results of isotopic datings performed on rocks from both units (Brueckner *et al.* 1996; O'Brien *et al.* 1997; Bylina *et al.* 2001; Dubińska *et al.* 2004). We will also compare the obtained virtual poles positions with the West Sudetic APWP and draw tectonic conclusions concerning the Sudetes.

2 GEOLOGICAL AND TECTONIC SETTING

The Góry Sowie Block (GSB) is the allochthoneous unit (Gordon *et al.* 2005) which, according to Franke & Żelaźniewicz (2000) can be assigned either to marginal parts of the Bohemian Massif incorporated into Devonian subduction-collision, or to units accreted to the northern margin of Bohemia during the Devonian. Presence of fragments of GSB rocks in the Frasnian-Fammenian Świebodzice Basin sediments proves that during the Late Devonian the GSB were already accreted to the West Sudetes (Porębski 1990). The JGSM is interpreted as a fragment of the dismembered Sudetic Ophiolite (Dubińska & Gunia 1997). The Sudetic Ophiolite probably represents a late stage extension of the Saxo-Thuringian Ocean and was accreted to the Sudetes in Late Devonian.

The GSB unit is essentially composed of migmatitic gneisses and minor granulites; it contains numerous small basic and ultrabasic bodies, generally with obscured contacts with the host migmatitic gneisses. The GSB ultrabasic xenoliths include harzburgite-orthopyroxenite with minor melanocratic norite (CIPW norm). The composition and habit of a relict Cr-spinel and olivine (Fo90) assemblage unequivocally prove the depleted mantle origin of ultrabasic rocks from GSB (Dubińska *et al.* 1999). GSB ultrabasic rocks clearly record metamorphic retrogression starting from eclogite facies conditions via amphibolite to subgreenschist facies metamorphism; the pT paths of gneisses and ultrabasic xenoliths from GSB are inconsistent (Dubińska *et al.* 2002).

The cooling age of the mantle-derived garnet-bearing peridotite from Bystrzyca Górna, GSB, was determined at 402 ± 3 Ma (Sm–Nd isochrone, Brueckner *et al.* 1996). This age is probably related to cooling of Sm–Nd decay system of the garnet below 650°C ± 30°C (Mezger *et al.* 1992). Metamorphic zircon from neighbouring mafic granulite records metamorphic peak of 775°C–900°C at 401 ± 1 Ma (Pb–Pb evaporation, O'Brien *et al.* 1997; Cherniak & Watson 2000). Extensive geochronometrical study of Zahniser (2004) revealed that GSB gneisses and amphibolites were cooled from 550°C to 380°C at *ca.* 390–372 Ma. Marheine *et al.* (2002) suggested that cooling <380°C of the central GSB continued up to 358 Ma. K–Ar determinations of the biotite from metasomatic Po (Fig. 1) contact zone revealed that gneisses of central GSB were cooled to *ca.* 350°C at *ca.* 344 Ma (Bylina & Banaś, private communication). The eastern side of the GSB yielded a Ar–Ar cooling age of *ca.* 337 Ma (muscovite & hornblende, see for details Zahniser 2004); this age is related to rapid heating and successively fast cooling caused by formation of the Niemcza shear zone. This geological episode is confirmed by Pb–Pb zircon age 334 ± 2 Ma; the zircon occurring from undeformed granodiorite sample from eastern block within the Niemcza shear zone (Kröner & Hegner 1998). Selected radiometric ages of GSB are shown in Fig. 2.

The Sudetic Ophiolite is represented by an almost complete ophiolite sequence according to the Penrose concept (Anonymous 1972). Three serpentinite massifs, adjacent to the GSB, are considered to be a dismembered mantle tectonite section (e.g. Majerowicz 1979; Dubińska & Gunia 1997). The JGSM, the largest of three ultrabasic bodies adjacent to GSB, is located close to its northern border. It displays different contacts with neighbouring geological units, that is, tectonic contacts with GSB gneisses and Ślęża metagabbro unit, the last being a fragment of the ophiolite sequence, and thermal contacts with Variscan granitoids of the Strzegom-Sobótka massif (e.g. Dubińska 1995). Unfortunately, there is no evidence of tectonic tilt in the study area which makes the fold test impossible. In the previous paper concerning palaeomagnetism of the Ślęża and Nowa Ruda ofiolite fragments (Jeleńska *et al.* 1995) we assumed them to be subhorizontal based on geological situation of the Fe–Ti enriched zone found by Jamrozik (1989) in the Ślęża complex. Now we assume that neither GSB nor JGSM were subjected to any tilting since about 390 Ma. The study area and sampling sites are shown in Fig. 1.

Peridotites (fresh or slightly altered) of JGSM are scarce and randomly distributed, while completely serpentinized rocks are frequent. Primary assemblages of ultrabasic rocks, roughly deduced on the basis of CIPW norm calculations combined with analysis of pseudomorphic varieties of serpentinites, suggest that serpentinites were predominantly formed at the expense of metamorphic harzburgites and lherzolites (Dubińska & Gunia 1997). The crystallization age of the ophiolite gabbros was determined at *ca.* 420 Ma (U–Pb zircon age, Oliver *et al.* 1993). Palaeomagnetic study of those gabbros were already performed (Jeleńska *et al.* 1995).

Initial serpentinization of JGSM ophiolite peridotite was directly dated at 400 +4/−3 Ma based on an integrated study of zircon from a rodingite blackwall (Dubińska *et al.* 2004).

3 SAMPLING AND EXPERIMENTAL METHODS

The studied rocks were collected as hand samples oriented with a geological compass in the localities presented in Fig. 1. Twenty-five hand samples of ultrabasic rocks were sampled in the 4 exposures of GSB: Potoczek (Po), Zagórze (Zag), Gilów (Gil) and Chmielina (Chm), see Tables 1 and 3. Apart from these samples additional two samples of eclogites and five samples of migmatitic gneisses were taken in Zag and five samples of gneisses were taken in Po. The ultrabasic rocks were sampled only in Gil and Chm occurrences. From three exposures in the JGSM 28 hand samples of serpentinites were taken (see Tables 2 and 3). In Jordanów (Jo), apart from serpentinites, four samples of neighbouring quartz-zoisite rocks were also sampled. From each hand sample, three to five specimens were drilled for palaeomagnetic and rock-magnetic purposes. We have also included the results obtained for nine hand samples of serpentinites taken few years ago in the exposure Kiełczyn (K in Fig. 2). Magnetic properties of the K rocks are thoroughly discussed in Kądziałko-Hofmokl (2001).

In the course of palaeomagnetic investigations we realized that results revealed for gneisses, eclogites and quartz–zoisite rocks are unreliable, therefore only results for ultrabasic rocks will be presented and discussed here. The numbers of hand samples of ultrabasic rocks taken in respective localities (from five to 17 in each locality) are summarized in Table 3. The difficulty of sampling and lack of

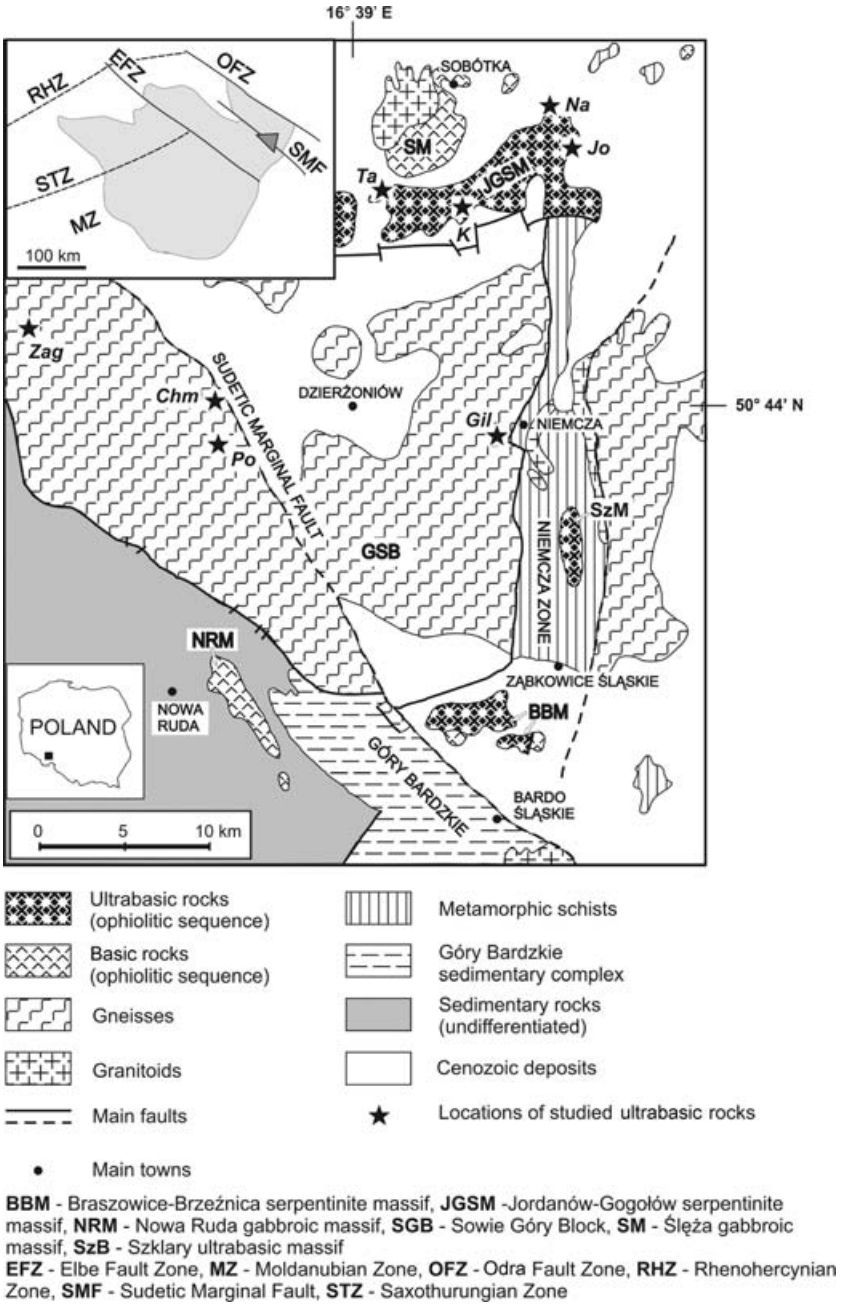

Figure 1. Geological sketch of Góry Sowie Block and Sudetic ophiolite (after Dubińska & Gunia 1997; Gunia 1997). Po—Potoczek, Zag—Zagórze Śląskie, Chm—Chmielina, Gil—Gilów, Na—Nasławice, Ta—Tpadła, Jo—Jordanów, K—Kiełczyn.

proper exposures limited the number of collected samples. However, we believe that for metamorphic rocks the number of samples corresponds to the sampling requirements summarized by Morris (2003) and adequately characterize the petrological and magnetic characteristics of investigated exposures.

Petrological and mineralogical studies were performed on specimens previously demagnetized by an alternating field. Backscattered electron (BSE) images and X-ray composition mappings were recorded using a CAMECA SX 100 electron microprobe.

Identification of minerals responsible for the magnetic properties of studied rocks was performed using two magnetic methods based on thermomagnetic measurements. (i) Thermal decay of saturation isothermal remanence (SIRM), and (ii) changes of bulk magnetic susceptibility (Kb) during heating.Measurements of SIRM acquired in high magnetic fields (3–7 T) were made during heating up to 700°C in a non-magnetic space using the TUS device (Poland, Kądziałko-Hofmokl & Kruczyk 1976). The SIRM versus temperature plots supplied values of blocking temperatures Tb of magnetic minerals present in the studied samples. Analysis of Kb variations was performed during heating up to 700°C using a KLY-3/CS3 device (Agico-Brno, Czech Republic). The Kb versus temperature plots yielded Curie temperatures (Tc) of magnetic minerals present in the studied samples and monitored the appearance of new magnetic phases created during heating. The parameters of magnetic hysteresis (Mrs—saturation remanence, Ms—saturation magnetization, Hc—coercivity, Hcr—coercivity of remanence) were obtained

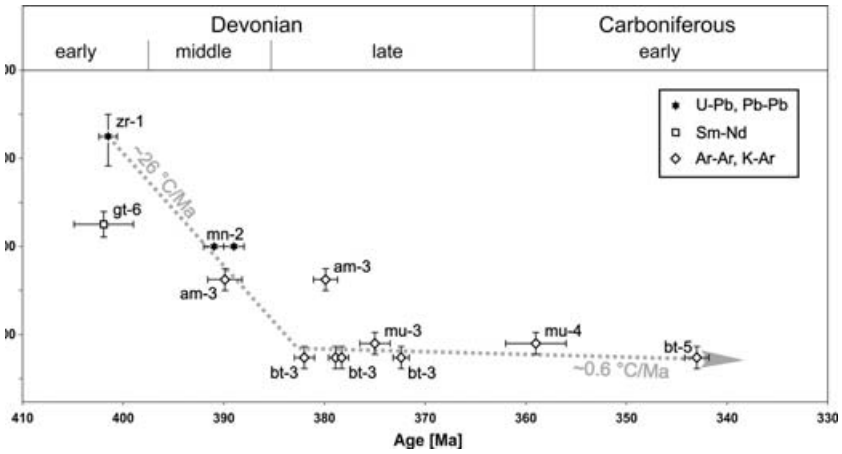

Figure 2. Temperature versus time diagram of northwestern and middle part of GSB; mineral abbreviations: am—amphibole, bt.—biotite, gt—garnet, mn—monazite, mu—muscovite, zr—zircon; sources: 1—O'Brien *et al.* 1997; 2—Bylina *et al.* 2001; 3—Zahniser 2004; 4—Marheine *et al.* 2002; 5—Bylina & Banaś (private communication); 6—Brueckner *et al.* 1996. The grey dotted arrow shows proposed exhumation rate of northwestern and middle GSB; assumed temperatures based on following sources: zr: Cherniak & Watson 2000, O'Brien *et al.* 1997; mn: Bylina *et al.* 2001; gt: Metzger *et al.* 1992; am: Harrison 1981; mu: Hames & Bowring 1994; bt: Grove & Harrison 1996.

using a Vibrating Sample Magnetometer (VSM, Molspin, UK). They were used for constructing Day plots (Mrs/Ms versus Hcr/Hc, *cf.* Day *et al.* 1977; Peters & Dekkers 2003) which supplied information about the dominating domain state of magnetic phases. For several samples, especially those in which the presence of maghemite coating of small magnetite grains was expected, hysteresis parameters were measured after consecutive heating steps from 100°C to 600°C. The obtained results were combined with mineralogical and petrological data.

The standard palaeomagnetic procedure consists of alternating field (AF) and thermal (TH) demagnetization of NRM. Intensity of NRM was measured using a SQUID (2G Enterprises, USA) cryogenic magnetometer after each demagnetizing step. AF demagnetization was performed using the 2G device integrated into the SQUID, with the highest demagnetizing field of 120 mT. TH demagnetization was done using a nonmagnetic furnace (Magnetic Measurements, UK). The samples were heated in steps from room temperature to 685°C, with temperature increment of 25° or 50°C. The measuring equipment is placed inside Magnetic Measurements compensating coils system; the magnetic field within the protected space did not exceed 5 per cent of the Earth's magnetic field. Phase transitions caused by heating in air during TH demagnetization were monitored by measuring the mean magnetic susceptibility (Km) after each heating step using KLY2/KLY3 bridges (Agico-Brno, former Geofyzika-Brno, Czech Republic). The demagnetization results were processed using the software package of Lewandowski *et al.* (1997) based on Kirschvink's (1990) principal component analysis and remagnetization circles method (Halls 1976). Several Zag specimens were additionally studied by applying combined analysis of remagnetization circles and direct palaeomagnetic observations (McFadden & McElhinny 1988).

4 RESULTS

4.1 Góry Sowie block (GSB)

4.1.1 Mineralogy and petrology

Ultrabasic xenoliths within GSB gneisses typically occur as small bodies up to *ca.* 100 m^2. Biotite-rich contact zones surrounding Po xenoliths suggest high-temperature emplacement into the GSB gneisses (ca. 600°C, Bylina *et al.* 2001).

The composition of the studied ultrabasic bodies (Table 1) varies from peridotite to pyroxenite, both containing relict (Al+Mg+Cr)-rich spinel and olivine. Their textural relationships and chemical compositions unequivocally indicate a pristine assemblage formation at *ca.* 1400°C (Dubińska *et al.* 1999). The xenoliths are usually intergrown by serpentine-group minerals, ±talc, ±magnetite, and ±Ni-sulphide (Table 1). The spatial relationships of antigorite and needle-shaped tremolitic amphibole and lizardite pseudomorphic replacements after both olivine and pyroxene suggest greenschist facies metamorphism overprinting an earlier serpentinization. Fe-hydroxide occurrences record a superficial alterations.

The peridotites from Zag and Chm are layered. The dark-grey layers are composed of relict olivine, bastitic pseudomorphs after pyroxene, and minor (Al+Mg+Cr)-rich spinel, whereas the light-grey layers are typically composed of Ca-amphibole ± clinopyroxene and orthopyroxene. The light-grey layers are younger as suggested by textural relationships; the chemical diversification of the amphiboles, pargasite to tremolite (according to classification of Leake *et al.* 1997), implies a HP-MT metamorphic event (Bylina *et al.* 2001). Gil pyroxenite contains following relict minerals: orthopyroxene, olivine, and (Al+Mg+Cr)-rich spinel.

The magnetic phases of GSB ultrabasic rocks consist of magnetite formed during serpentinization of ultrabasic rock (three generations), pyrrhotite, haematite (martite), and Fe-hydroxides. The oldest magnetite variety occurs in 'flame chlorite', ordered intergrowth of chlorite and magnetite (Fig. 3). The shape of 'flame chlorite' aggregates suggests a pseudomorphic replacement after an unidentified Fe, Al-rich silicate phase (i.e. surassite).

The second generation of magnetite formed as a result of pyrrhotite oxidation related to the serpentinization process (Fig. 3) analogously to Frost's (1985). This magnetite variety was found exclusively in Zag samples. The youngest magnetite generation forms euhedral crystals within serpentine pseudomorphs, veinlets and irregular aggregates (Fig. 3). There are two generations of pyrrhotite. The early generation is a product of (Fe+Ni)-monosulphide decomposition during metamorphic retrogression; it contains ca.1 per cent Ni; the younger generation of pyrrhotite is Ni-free. The early pyrrhotite variety is mostly replaced by the second generation of

Table 1. Petrological characteristics of studied rocks from GSB.

Locality	Rock-type mineralogy	Processes below 600°C typical newly formed minerals	Magnetic minerals
Chmielina	Layered metaperidotite (MT-MP) *Light-grey layer*: tremolitic amphibole (locally replaced by lizardite), bastite[a]; *dark-grey layer*: bastite[a], relict olivine (Fo88), (Al+Mg+Cr)-rich spinel (surrounded by ferrichromite);	Retrograde overprint, closed-system serpentinization lizardite, chrysotile, brucite, andradite, tremolitic amphibole, magnetite, Ni-sulphides, calcite, flame-shaped chlorite[b]	magnetite
Gilów	Pyroxenite relict orthopyroxene, relict olivine, relict (Al+Mg+Cr)-rich Spinel, bastite[a]	Serpentinization, greenschist metamorphic overprint, low-temperature alteration (weathering) lizardite, chrysotile, antigorite, flame-shaped chlorite[b], fan-shaped tremolite aggregates, haematite (martite), Fe-hydroxides	magnetite, haematite (martite), Fe-hydroxides
Potoczek	Spinel peridotite olivine (Fo88), enstatitic orthopyroxene (porphyroclasts), (Al+Mg+Cr)-rich spinel (interstitial and inclusions in orthopyroxene);	Granulite-facies metamorphism with retrograde overprint, combined with K,Al-metasomatism, and subsequent low-temperature alteration amphiboles (pargasite-to-tremolite, late actinolite), lizardite, chrysotile, magnetite, pyrrhotite, flame-shaped chlorite[b], talc, Fe-hydroxides	magnetite, pyrrhotite, Fe-hydroxides
Zagórze Śląskie	Layered metaperidotite (MT-HP) *Light-grey layer*: amphibole (magnesiotaramite-to-pargasite), orthopyroxene, clinopyroxene, hercynite, Mg-biotite (acc.); *dark-grey layer*: olivine (Fo86-88), flame-shaped chlorite[b] with (Al+Mg+Cr)-rich spinel inclusions, single amfibole, pentlandite (acc.), apatite (acc.);	Retrograde overprint lizardite, talc, graphite, magnetite, pyrrhotite	magnetite, pyrrhotite

[a]Pseudomorphic lizardite replacement after pyroxene.
[b]Chlorite-magnetite. intergrowths, Fo—forsterite end-member content, acc.—accessory.

Table 2. Petrological characteristics of studied rocks from JGSM.

Locality	Rock type mineralogy	Processes below 600° C typical minerals	Magnetic minerals
Jordanów Śląskie	Antigorite serpentinite developed in expense of pseudomorphic serpentinite *Major minerals*: antigorite, magnetite; *minor minerals*: relict (Al+Mg+Cr)-rich spinel, chrysotile (in veins), lizardite, Ni-sulphides, talc, carbonates, Nephrite with metarodingite clast	Greenschist metamorphic overprint, low-temperature alteration (weathering) antigorite, haematite (martite), Fe-hydroxides Greenschist metamorphic overprint, low-	magnetite, haematite (martite), Fe-hydroxides pyrrhotite,
	Major minerals: cataclased albitic plagioclase, andraditic garnet, tremolitic amphibole (fibrous and prismatic, nephrite?); *minor minerals*: relict rutile (zonally overgrown by ilmenite and titanite), zoisite, K-feldspar, clinopyroxene, magnetite, pyrrhotite	temperature alteration (weathering) tremolitic amphibole, Fe-hydroxides	magnetite, Fe-hydroxides
Nasławice	Pseudomorphic serpentinite formed in expense of peridotite *major minerals*: lizardite, chrysotile, magnetite; *minor minerals*: relict (Al+Mg+Cr)-rich spinel, antigorite, Ni-sulphide	Serpentinization, low-temperature alteration (carbonate formation) lizardite, chrysotile, Mg,Ca-carbonates	magnetite
	Antigorite serpentinite after pseudomorphic serpentinite *Major minerals*; antigorite, chrysotile (in veins), magnetite;; *minor minerals*: relict (Al+Mg+Cr)-rich spinel, lizardite, Ni-sulphides;	Greenschist metamorphic overprint, low-temperature alteration (carbonate formation antigorite, Mg,Ca-carbonate	magnetite
	Serpentinite conglomerate *Clasts*: pseudomorphic serpentinite, antigorite serpentinite, fine-grained serpentinite, fragments of chrysotile veinlets, grains of (Al+Mg+Cr)-rich spinel; *matrix*: lizardite overgrown by antigorite, magnetite, carbonates;	Greenschist metamorphic overprint antigorite	magnetite
Tąpadła	Cumulate dunite olivine (Fo90-91, with {100} partings), magnetite (inclusions in olivine), bastite[a]	Serpentinization, greenschist metamorphic overprint, low-temperature alteration (weathering) chlorite, lizardite, antigorite, tremolitic amphibole (fibrous and prismatic), Ti-bearing ferrichromite, talc, carbonates, Fe,Ni-sulphides, Ni-sulphides, Fe-hydroxides	magnetite, Fe-hydroxides

Note. For explanations see Table 1.

Table 3. Magnetic characteristics of sampled rocks.

Exposure	Lithology	*N*	Kmx10^{-3}SI	NRM mA m^{-1}	Ms mA m^{-2}	Mrs mA m^{-2}	Hc mT	Hcr mT
Potoczek Po	Spinel peridotite	5	4.5–20	200–1300	0.13–0.75	0.03–0.25	13–20	20–35
Zagórze Zag	Layered peridotite	5	21–1300	500–1400	2–6.5	0.48–0.7	6 -18	16–20
Gilów Gil	Pyroxenite	6	90–170	5200–9300	4–9	0.4–0.8	5.5–8.5	12–25
Chmielina Chm	Layered metaperidotite	7	16–108	2800–9900	1.5–4.5	0.35–0.78	10.5–17.5	20–25
Nasławice Na	Serpentinite	9	20–120	500–2500	1.5–6	0.06–0.33	4–9.5	15–40
	Serpentinite Conglomerate	8	50–140	700–2000	5–11	0.15–0.65	3–4.5	8.5–24
Jordnów Jo	Antigorite serpentinite	5	60–110	1400–2600	4.8–6.2	0.2–0.4	4–5	12–16
Tąpadła Ta	Cumulate dunite	7	11–190	200–3000	1.5–2.8	0.1–0.55	2.5–10	9–17
Kiełczyn K	Serpentinite	9	29–76	450–4150	*ca.* 0.7	*ca.* 0.07	*ca.* 8	*ca.* 20

Exposure—names and abbreviations of exposures, N—number of hand samples taken in the field, Km—mean susceptibility, NRM—intensity of natural remanence, Ms—saturation magnetization, Mrs—saturation remanence, Hc—coercivity, Hcr—coercivity of remanence.

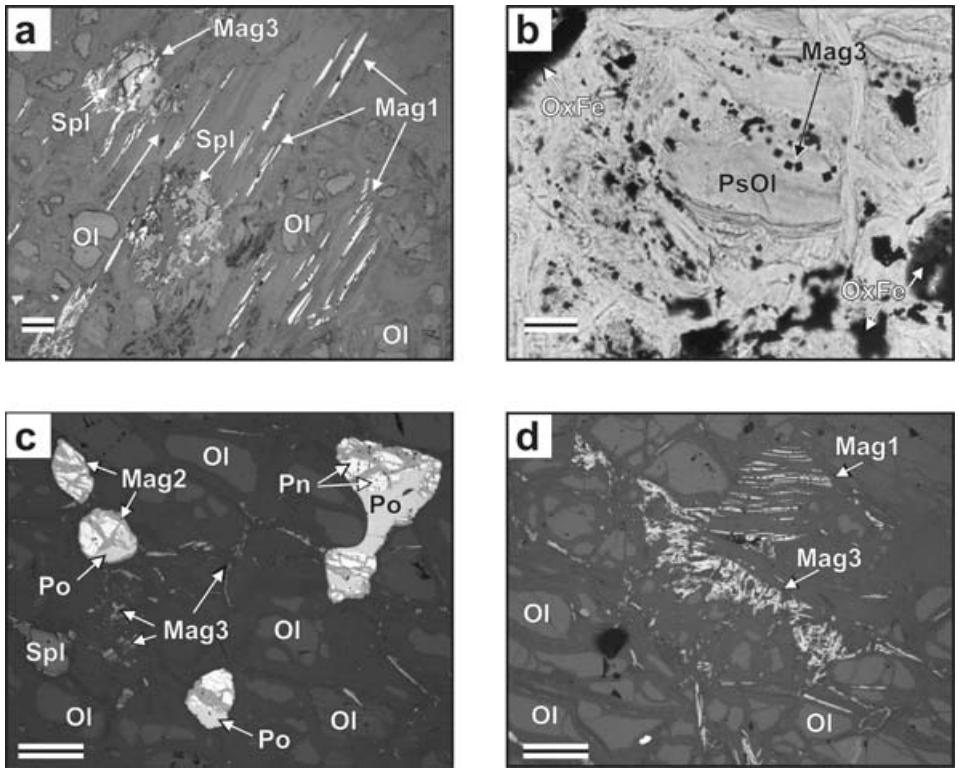

Figure 3. Microphotographs of ultrabasic rocks from Góry Sowie block; (A) Partially serpentinized ultrabasic rock (mush texture) with relict olivine and (Al+Mg+Cr)-rich spinel, containing 'flame chlorite' and generation of magnetite genetically related to serpentinization process; sample Po47; polarizing microscope, reflected light, one polar. (B) Serpentinite with pseudomorphic replacements after olivine containing idiomorphic magnetite overprinted with Fe-hydroxides; sample Po41a1; polarizing microscope, transmitted light, one polar. (C) Partially serpentinized ultrabasic rock (mush texture) with relict olivine, (Al+Mg+Cr)-rich spinel and pyrrhotite–pentlandite grains containing older magnetite generation within the fissures; sample Zag11; polarizing microscope, reflected light, one polar. (D) Partially serpentinized layered metaperidotite (dark-grey layer) with numerous relict olivine grains (mesh texture), containing 'flame chlorite' and the youngest generation of magnetite genetically related to serpentinization process; sample Zag 21, polarizing microscope, reflected light, one polar. Mag1—magnetite intergrown with chlorite ('flame chlorite'), Mag2—magnetite formed due to pyrrhotite oxidation (seemingly connected to the serpentinization process), Mag3—magnetite genetically related to serpentinization process, Ol—olivine (relict), OxFe—Fe-hydroxide, Pn—pentlandite, Po—pyrrhotite, PsOl—pseudomorphic replacement after olivine, Spl—(Al+Mg+Cr)-rich spinel. Scale bar = 200 μm.

magnetite and pentlandite (Fig. 3). The late pyrrhotite seems to be formed due to a local increase of sulphur activity during alteration of early sulphides. Martite (haematite) and Fe-hydroxides are frequent products of low-temperature alteration.

4.1.2 Rock-magnetic study

The thermomagnetic results confirm the prevailing content of magnetite (Tb 560°C–585°C) in rocks from all studied localities (Fig. 4a). The high-temperature segments of SIRM–T curves for Zag and Gil (Figs 4b and c) do not reveal a mineral with higher Tb, whereas in several specimens from Po, the prevailing magnetite is accompanied by a minor content of magnetic phase displaying Tb of *ca.* 610°C–620°C (Fig. 4d), probably maghemite. The Kb–T curve for Po (Fig. 4e) supports this conclusion. The Kb–T plot for Chm reveals only magnetite. Pyrrhotite observed in Po and Zag samples in reflected light (Table 1), is probably non-magnetic because it did not appear on thermomagnetic curves. In numerous Po and Gil

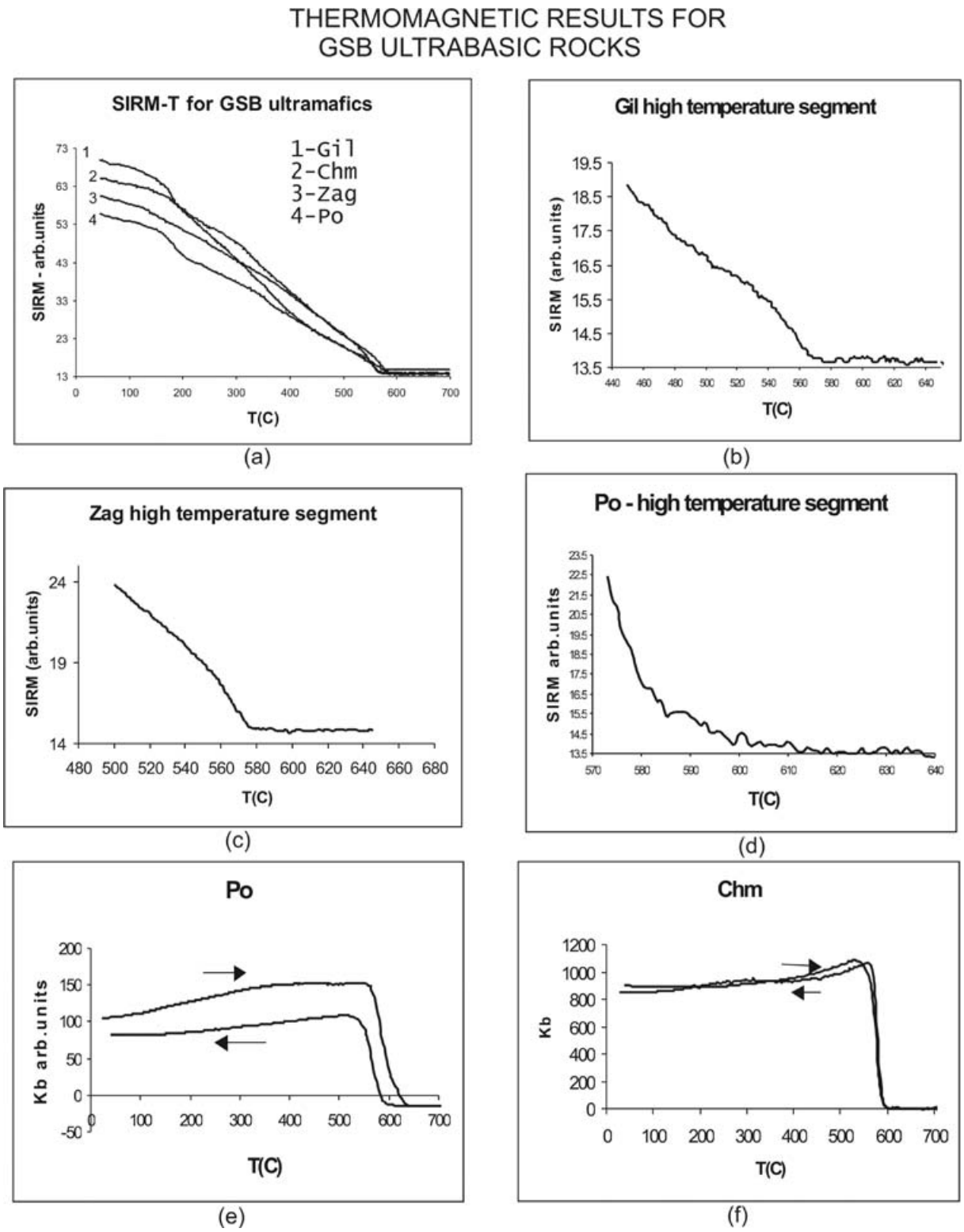

Figure 4. Thermomagnetic results for ultrabasic rocks from the GSB (a)—SIRM–T curves typical for Gil, Chm, Zag and Po (b), (c), (d) high-temperature segments of the SIRM–T curves for the Gil, Zag and Po specimens, respectively (e) Kb–T plot for Po specimen (f) Kb–T plot for Chm specimen.

specimens the SIRM–T curves reveal a slight decrease of remanence between 170°C and 200°C (Fig. 4a). This effect can be due to the presence of goethite, which was observed microscopically.

Mean susceptibility Km (Table 3) attains lower values in Po spinel peridotites (4.5–20×10–3SI) than in rocks from Gil and Chm. The layered peridotites from Zag display the great scatter of Km values, perhaps due to their inhomogeneity (Table 3). During step heating Km remains relatively stable up to 550°C in Zag, and up to 670°C in Gil, Chm and Po samples. In higher temperatures Km decreases due to oxidation of magnetite to haematite, (Figs 5a and b).

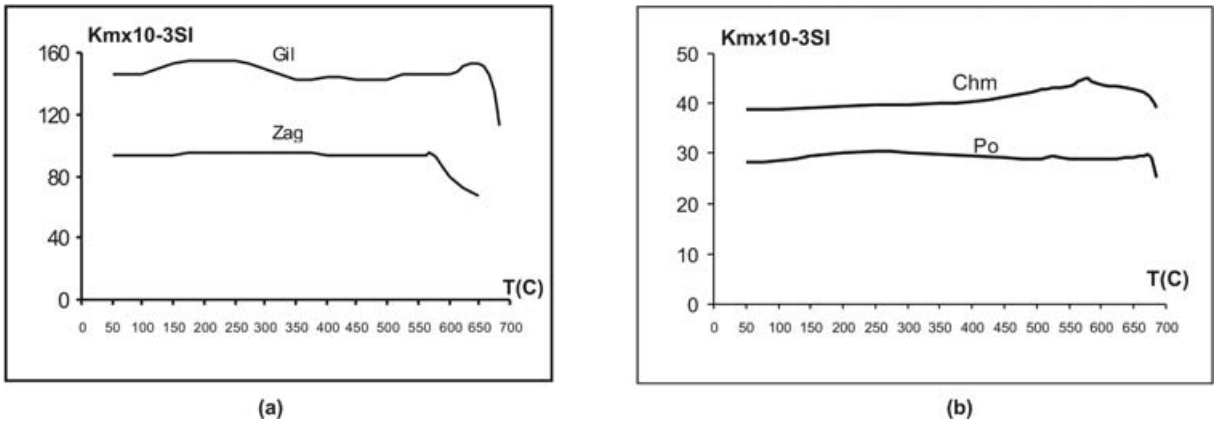

Figure 5. Km–T curves for ultrabasic rocks from GSB (a) Gil and Zag specimens (b) Chm and Po specimens.

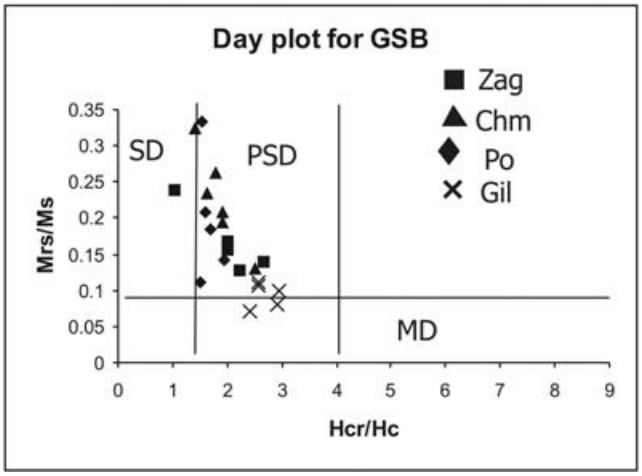

Figure 6. Day plot for ultrabasic rocks from GSB.

The values of hysteresis parameters are included in Table 3. Mrs, Ms, Hc and Hcr are characteristic for magnetite-rich rocks. The Day-plot (Fig. 6) indicates that magnetite occurs essentially in a PSD state corresponding to the results presented by Dunlop (2002) for serpentinized peridotites.

4.2 The Jordanów–Gogołów Serpentinite Massif (JGSM)

4.2.1 Mineralogy and petrology

The JGSM ultrabasic rocks, (serpentinites, Table 2) represent different textural types: pseudomorphic lizardite±chrysotile serpentinites, non-pseudomorphic antigorite variety, chrysotile asbestos, lizardite rosette serpentinites, etc. Their distribution is irregular; blocks and boudins of pseudomorphic serpentinites adjoin both a variety highly obliterated by antigorite blades and ubiquitous serpentinite mylonite wedges.

Studied rocks from Na comprise pseudomorphic variety of serpentinite, antigorite variety developed at the expense of pseudomorphic serpentinite, and serpentinite conglomerate composed of various serpentinite clasts cemented by fine-grained lizardite with antigorite laths overprinting both clasts and matrix. The serpentinite textures and mineralogy suggest that early low-temperature serpentinization, which produced lizardite±chrysotile pseudomorphic serpentinites was extensive, while posterior recrystallization producing massive antigoritic serpentinites was less frequent (Dubińska 1995). Samples from Jo represent antigorite serpentinite and nephrite with metarodingite clasts (Table 2). Magnetite, the main magnetic phase in Na and Jo samples, was formed during serpentinization. The magnetite occurs as partial or/and complete replacements after primary holy-leaf spinel, separate aggregates, scattered fine grains, and veinlets (Fig. 7c). Martite (haematite/maghemite) can be a product of low-temperature magnetite alteration (Fig. 7d).

The cumulate dunite from Ta (Table 2) contains abundant olivine often with 'magnetite dust' and magnetite replacements after primary and bastitic pseudomorphs after interstitial pyroxene (Figs 7a and b). Frequent interstitial chlorite aggregates probably were formed at the expense of primary plagioclase. Numerous late tremolite blades indicate greenschist facies metamorphic overprint. Silicate spinel decomposition (ca. 12 GPa & 1200°C according to Liou *et al.* 1998) is a tentative explanation of the olivine-magnetite intergrowths. Primary spinels (Spl, e.g. $(Fe^{3+}_{1.48}Al_{7.28}Cr_{7.09}V_{0.06}\ Ti_{0.14})$ $(Fe^{2+}_{4.02}Mg_{3.62}Mn_{0.13}Zn_{0.16}Ni_{0.02})\ O_{32}$) from Ta cumulate dunite than are partially altered through Fe–Cr spinel (Fe, Cr spl, e.g. $(Fe^{3+}_{8.30}$ $Al_{0.42}Cr_{7.06}\ V_{0.04}Ti_{0.25})$ $(Fe^{2+}_{6.43}Mg_{1.18}Mn_{0.21}Zn_{0.03}Ni_{0.09})\ O_{32}$) into magnetite (Mag3, Fig. 8). Optical microscopy and BSE images performed for K serpentinites (Kądziałko-Hofmokl 2001) revealed presence of fine magnetite grains formed during serpentinization, post-magnetite haematite (martite), and numerous chromite grains often partly altered to magnetite.

4.3 Rock-magnetic study

The characteristic SIRM thermal decay curves for Ta, Jo, and Na samples are shown in Fig. 9(a). In Ta (cumulate dunite), the high-temperature segment of the SIRM–T curve (Fig. 9b) and Kb–T plot (Fig. 9d) prove the presence of two magnetic phases—magnetite with Tb *ca.* 570°C and Tc *ca.* 580°C, and a second phase with Tb *ca.* 510°C and Tc *ca.* 540°C. The same two Tc values were observed in the K specimens (Kądziałko-Hofmokl 2001). The phase with lower Tb(Tc)is probably caused by ferrichromite, a magnetic Fe–Cr spinel. Schmidbauer (1969, 1971) determined Tc of ferrichromite $x = 0.7$ and $x = 1$, *ca.* 370°C, and *ca.* 200°C, respectively. Tc depends on multiple factors, that is, degree of ferrichromite oxidation, Mg and Al content, and internal stress. Therefore determination of x through the Tc values is problematic. Fernandes (1999) described ferrichromite that revealed Tc between 100°C and 533°C.

The Hopkinson effect observed in the Ta sample on Kb–T plot (Fig. 9c) indicates that the phase with lower Tc occurs in

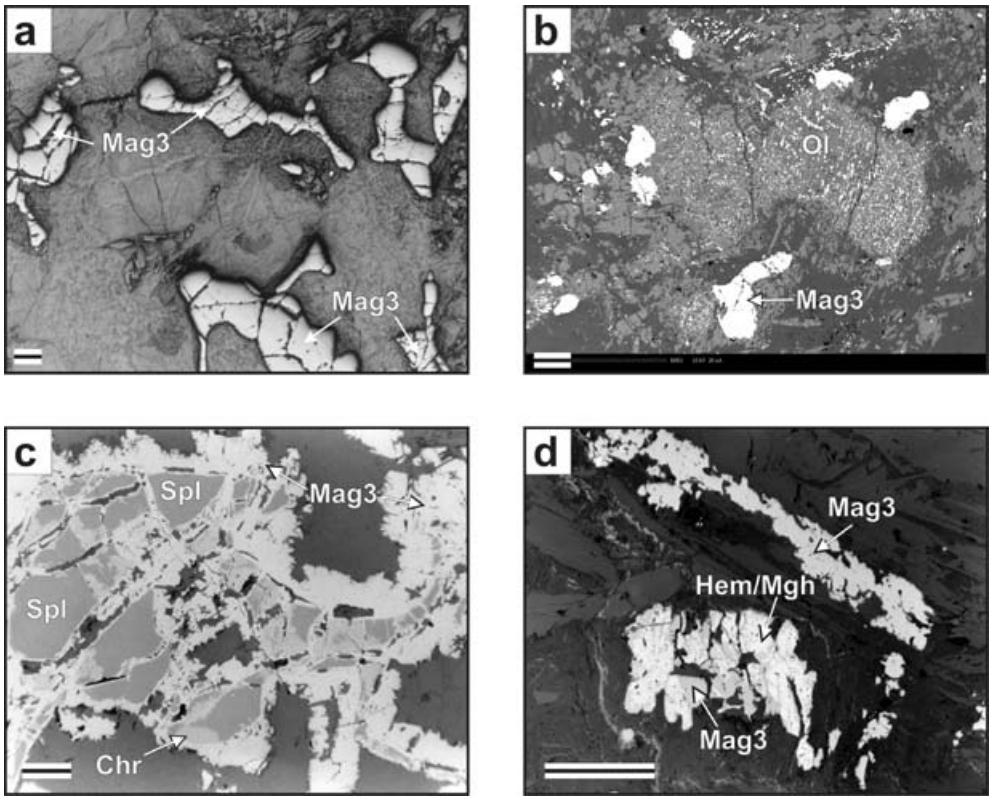

Figure 7. Microphotographs of ultrabasic rocks from JGSM; (A) Partially serpentinized cumulate dunite with magnetite replacements after primary holy-leaf spinel; sample Ta16; polarizing microscope, reflected light, one polar. (B) Weakly serpentinized cumulate dunite containing olivine grain with numerous magnetite inclusions ('magnetite dust') and large magnetite aggregates; sample Ta16; BSE image. (C) Pseudomorphic serpentinite; altered (Al+Mg+Cr)-rich spinel with chromite zones, surrounded by newly formed magnetite; sample KD-Na2; polarizing microscope, reflected light, one polar. (D) Antigorite serpentinite developed in expense of pseudomorphic serpentinite; large magnetite aggregates partially altered into martite (haematite); sample Jo77b2; polarizing microscope, reflected light, one polar. Chr—chromite, Hem—haematite, for other abbreviations see Fig. 2. Scale bar = 200 μm.

well-crystallized grains (Dunlop 1974). The Hopkinson peak appears neither on the cooling curve, nor on the curves of second heating and cooling, meaning that superparmagnetic grains were formed due to heating. The mean susceptibility Km for Ta rocks hardly changes up to *ca.* 700°C (Fig. 10).

In the majority of Jo specimens, magnetite is the only phase discernible on the SIRM–T curves, but sometimes it is accompanied by a small amounts of haematite or maghemite observed on the high-temperature segment of the SIRM–T curves (Fig. 9c) and on the Kb–T plots as Kb characteristic decreases during heating between 250°C and 450°C, (Fig. 9e). This hump reflects inversion of maghemite, present in the rock, into haematite (Orlicky 1990, 1994). Small hump at 250°C–300°C appearing on Km-T plots of Jo specimens supports conclusion of maghemite presence (Fig. 10).

The SIRM versus T plots for Na serpentinites show an inflection point at the temperature *ca.* 200°C where SIRM partly decreases. Moreover, SIRM importantly decreases at the Tb temperature *ca.* 370°C. The magnetite with Tb of 580°C occurs here only as a minor component (Fig. 9a). Heating to 200°C suppresses the first decrease of SIRM leaving only the higher Tb's (see inset in Fig. 9a). The Kb versus T plot (Fig. 9f) shows a significant increase of susceptibility in the range of 200°C–300°C, quick decrease up to 400°C caused by inversion of maghemite to haematite (Orlicky 1990, 1994) and run characteristic for magnetite with Tc *ca.* 580°C. Km–T plot (Fig. 10) reveals an increase of Km between 200°C and 350°C followed by its decrease, due to the presence of maghemite.

The thermomagnetic behavior of Na samples reminds the observed earlier behavior of the K rocks (Kądziałko-Hofmokl 2001). In order to explain the Na results, the parameters of hysteresis were measured for several specimens after consecutive heating steps during heating to 600°C. The experiments recorded an increase of Ms and simultaneous decrease of Mr and Hc in the same temperature range of 200°C–300°C, in which the increase of Kb on the Kb versus T curve was observed (Fig. 12), as for the K rocks, quoted above. The results obtained for Na indicate that here, as in K, fine grains of surface–oxidized magnetite into maghemite are present (Kądziałko-Hofmokl 2001). A thin maghemite coating on fine magnetite grains generates stress which increase coerciviy and remanence, as well as diminish susceptibility and magnetization (Gapeev *et al.* 1991; van Welzen 1992; Dunlop & Őzdemir 1996; Kądziałko-Hofmokl 2001). Heating samples to 200°C reduces strains in magnetite due to destruction of a maghemite coating. As a result the inflection point at 200°C disappears on SIRM *versus*T curves, susceptibility and magnetization increase while coercivities and remanences decrease. According to van Welzen (1992) this type of oxidation proceeds at low temperatures, even at a weathering conditions. Magnetite grains that loose their maghemite coating, oxidize differently during successive heating. An abundant phase with Tb *ca.* 370°C found in Na samples was tentatively identified as maghemite. Its presence supports increase of Kb at 150°C–250°C coupled with destruction of the maghemite coating, and results in Hopkinson peak formation at *ca.* 300°C. Haematite and goethite are minor magnetic phases in Na rocks.

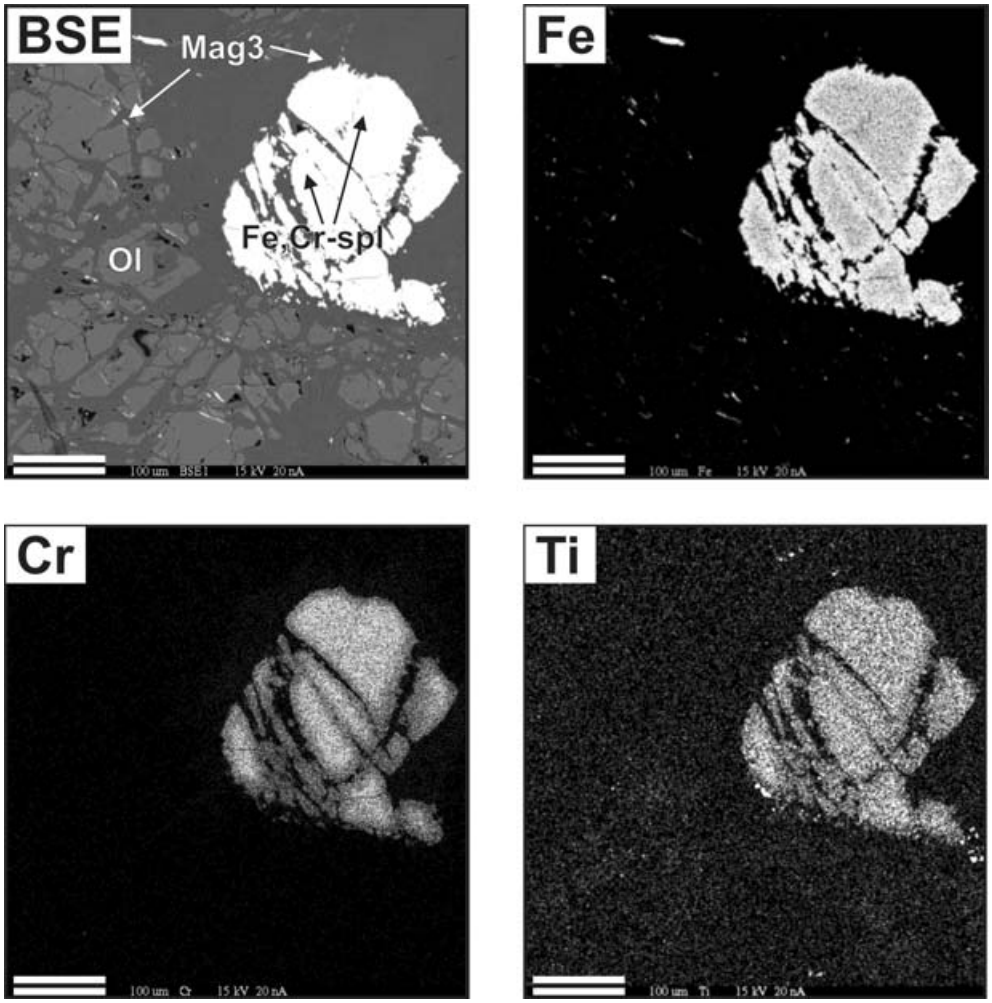

Figure 8. Altered ferrichromite (Fe,Cr-spl) from cumulate dunite surrounded by third generation of magnetite; sample Ta14b; BSE image and X-ray compositional maps (Kα lines); note the Fe and Cr zoning of ferrichromite. Fe,Cr-spl—ferrichromite, Mag3—magnetite, third generation, Ol—olivine, scale bar = 100 μm.

The values of hysteresis parameters obtained for studied localities are close to the values obtained for GSB ultrabasic rocks (Table 3) and are typical for magnetite/maghemite rich rocks, although the Day plot is different that the plot for the GSB. According to the Dunlop interpretation of the Day plot (Dunlop 2002) magnetite occurs essentially as PSD grains in the case of Ta and Jo, while Fe-oxides in Na occur in PSD and MD states or as mixture of SD and MD with addition of SP grains (Fig. 11).

5 PALAEOMAGNETIC RESULTS

The values of NRM intensity together with the other magnetic parameters described in the previous section are included in Table 3. Selected demagnetization diagrams for each exposure are displayed in Figs 13(a)–(f) and 14(a)–(h). The stereographic plots of directions of isolated characteristic NRM components are shown on Figs 15(a)–(h).

5.1 Góry Sowie Block (GSB)

Potoczek (Po). Demagnetization experiments were performed for 19 specimens (8 AF, 11 TH). The demagnetization results show rather low median destructive field MDF (about 10 mT) and very clearly, the presence of two components of NRM: one of lower stability (0–10 mT) labelled PoA2 and another one with higher stability, labelled PoA3 (Fig. 13a). Intensity of NRM often increases after demagnetization at 50–60 mT forbidding determination of demagnetizing field. Thermal cleaning was less effective; it usually revealed one high-temperature component with Tub of magnetite (550°C–575°C), usually corresponding to the component PoA2 revealed with AF demagnetization. Nevertheless, in a few cases, we were able to find a component, which demagnetized in temperatures characteristic for magnetite (575°C–600°C) and had a direction corresponding to the direction PoA3 revealed by AF cleaning (Fig. 13b). Both characteristic components have SW declinations and low positive and negative inclinations in PoA2, and high-intermediate positive inclinations in PoA3 (Fig. 15a).

Zagórze Śląskie (Zag)—the sampled blocks of ultrabasic rocks differ from each other macroscopically—only one of them is uniformly dark, the other four are light with dark stripes. This inhomogeneity is reflected in very variegated values of Km and intensity of NRM (Table 3). Demagnetization experiments were performed for 21 specimens (2 AF, 19 TH). Specimens demagnetized quickly by the AF method—MDF is about 5 mT (Fig. 13c). The thermal cleaning curves show a monotonous decrease of NRM up to

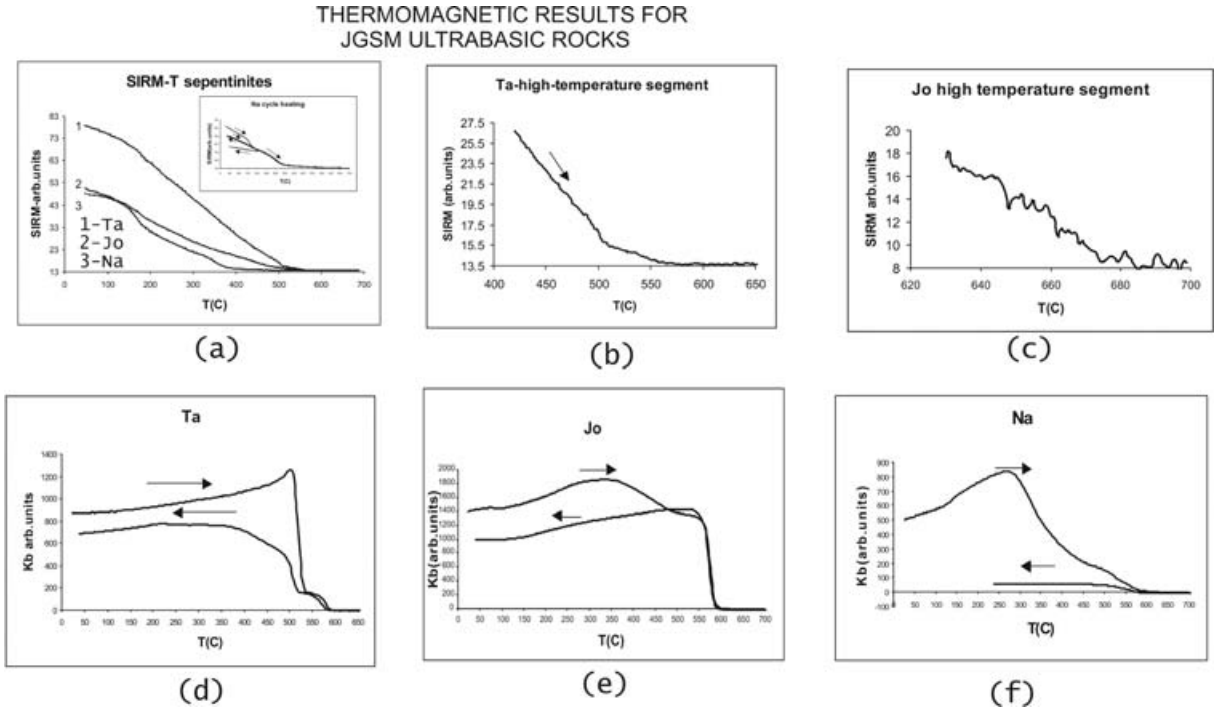

Figure 9. Thermomagnetic results for ultrabasic rocks from the JGSM (a)—SIRM–T curves typical for Ta, Jo and Na specimens, inset shows results of cycle heating of Na specimen (b), (c) high-temperature segments of the SIRM–T curves for the Ta and Jo specimens, respectively (d), (e), (f) Kb–T plots for Ta, Jo and Na specimens, respectively.

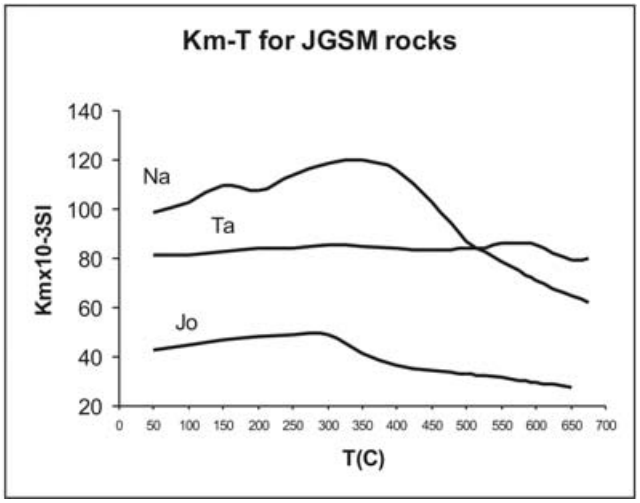

Figure 10. Km–T plots for ultrabasic rocks from JGSM.

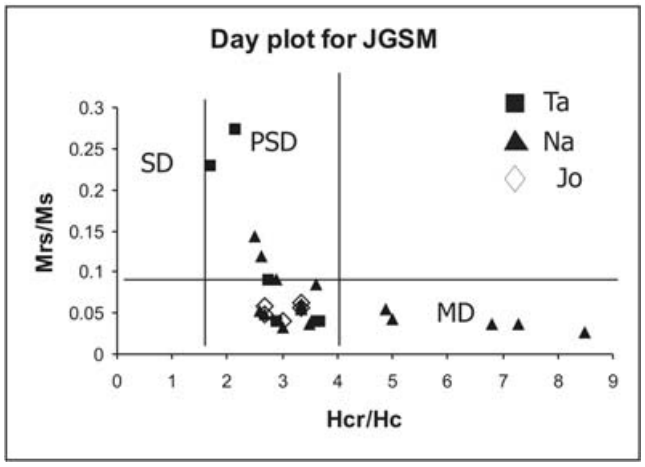

Figure 11. Day plot for ultrabasic rocks from JGSM.

575°C–600°C and a sudden drop to about 1 per cent or less of its primary value after heating to 625°C (Fig. 13d). This characteristic implies the presence in these rocks not only of magnetite with Tb revealed by thermomagnetic experiments but also small amount of another phase. In the majority of specimens two NRM components were isolated either as lines fitted to segments of demagnetization plots, or as Hoffman-Day directions, or as results of combined analysis of remagnetization circles and direct palaeomagnetic observations of McFadden & McElhinny (1988).

The directions of isolated components show an important scatter often even between specimens coming from the same sample. Nevertheless, we found among them directions forming cluster observed unmistakably in Po as component A3 and labelled it as A3 component as well (Table 3, Fig. 15b).

Gilów (Gil)—the intensity of NRM is rather homogenous and considerably lower than in the remaining GSB ultrabasic rocks (Table 3). Out of 18 demagnetized specimens 12 were cleaned thermally and 6 with AF. The AF demagnetization curves show that NRM of the Gil rocks have low and inhomogeneous stability (MDF varies from 3 to 10 mT). The curves revealed dominance of characteristic component GilA1of N declinations and negative or positive low inclinations, sometimes associated or replaced by the second component GilA2 of W declination and low negative or positive inclinations (Fig. 15c). Both are isolated in fields of various intensities, from low *ca.* 10 mT to high 60–120 mT (Fig. 13e). Thermal cleaning

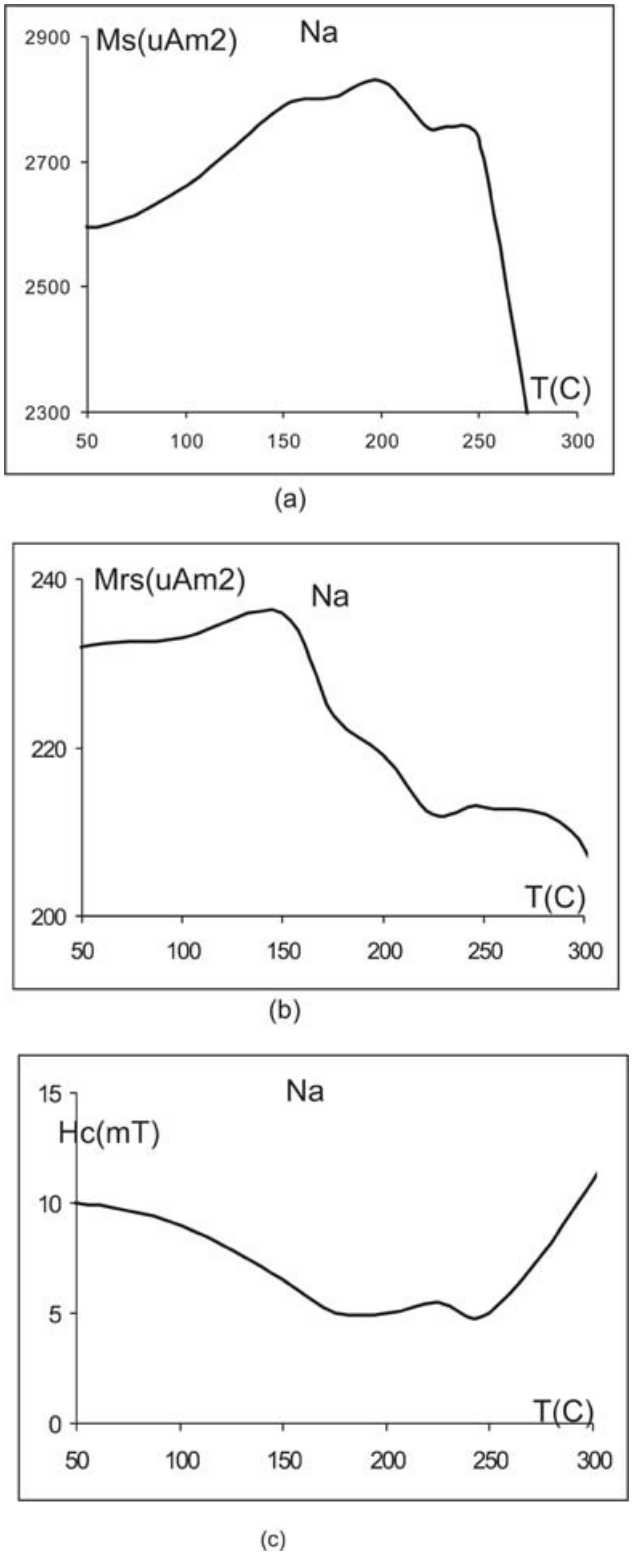

Figure 12. Changes of hysteresis parameters of Na specimen during step-like heating (a) saturation magnetization Ms, (b) saturation remanence Mrs, (c) coercivity Hc.

usually shown one component either GilA1 or GilA2 isolated as a line usually ranging from 50°C–250°C to 650°C–675°C.

Chmielina (Chm)—20 specimens were demagnetized (13 TH,7 AF). The AF demagnetization curves yield MDF of 7 mT; in the majority of specimens the intensity of NRM increases after application of 30–40 mT. In most specimens the main part of NRM becomes demagnetized in unblocking temperatures characteristic for magnetite, as expected from thermomagnetic analysis (Fig. 13f). In some specimens after heating to 575°C, a large part (even 40 per cent) of NRM remained and became completely demagnetized only after heating to temperatures exceeding 600°C, implying that an important part of NRM is carried by maghemite/haematite. Numerical analysis of demagnetization data shows the presence of characteristic components of southern declinations and low to high positive and negative inclinations (Fig. 15d). Despite the scatter of the directions we have treated them as two clusters and calculated two components: ChmA1 with S declination and positive intermediate inclinations and ChmA with similar declination and negative intermediate inclination (Table 3).

5.2 Jordanów–Gogołów Serpentinite Massif (JGSM)

Nasławice (Na)—the intensities of NRM of all specimens are similar (Table 3). Demagnetization procedures performed on 19 specimens (13 TH and six AF) yielded MDF of about 7–10 mT. In higher fields the intensity of NRM monotonously decreases (Fig. 14a). Heating demagnetizes about 90 per cent of NRM in unblocking temperatures of about 350°C–400°C (Fig. 14b)—close to the prevailing Tb observed in these rocks. Numerical analysis revealed domination of one component with NW–NE declination and high positive inclination, labelled R, although in a few specimens components with SW declination and intermediate, positive and negative inclinations were also observed (Fig. 15e).

Jordanów Śląski (Jo)—the intensity of NRM of serpentinites is high and close to that observed in the Na rocks (Table 3). Analysis of TH (11 specimens) and AF demagnetization procedures (four specimens) revealed the presence of either one or two NRM components in each specimen (Fig. 14 c, d): one with NE declinations and intermediate–high positive inclinations isolated in unblocking temperatures 350°C–450°C, rarely 500°C, labelled Tr, and another one isolated in higher Tub (up to 575°C) with SSW declinations and positive intermediate inclinations, labelled JoA (Fig. 15f).

Tąpadła (Ta)—the intensity of NRM of cumulate dunites varies, as does the Km (Table 3). Demagnetization experiments carried out on 29 specimens (22 TH and 7 AF) show that NRM demagnetizes very quickly in an alternating field—the MDF is about 2.5 mT (Fig. 12e). Often after application of fields of 30–40 mT, NRM increased slightly. Numerical analysis revealed two components of NRM in each demagnetized specimen: a component labelled TaA1 with N–SE declinations and low positive inclinations in the low AF range (0–7 mT) and a component labelled TaA3 with S–SW declinations and intermediate positive inclinations in higher fields. During thermal cleaning the intensity of NRM decreased slowly up to 550°C–575°C, where it dropped down to few percent of its initial value, and became fully demagnetized at 600°–625° (Fig. 14f). Numerical analysis revealed the presence of two components of remanence in each specimen but their directions did not form clear clusters, as was the case with AF results. Nevertheless, we were able to discern component TaA3 with Tub reaching 500°C–600°C, component TaA1 for which Tub remaining in the range of 250°C–600°C, and component R for which Tub were of the same range. This component was not recorded with the AF cleaning (Fig. 15g).

Kiełczyn (K)—the intensity of NRM varies whereas the mean susceptibility Km is rather stable (Table 3). Demagnetization experiments were carried on 15 specimens, 13 specimens were

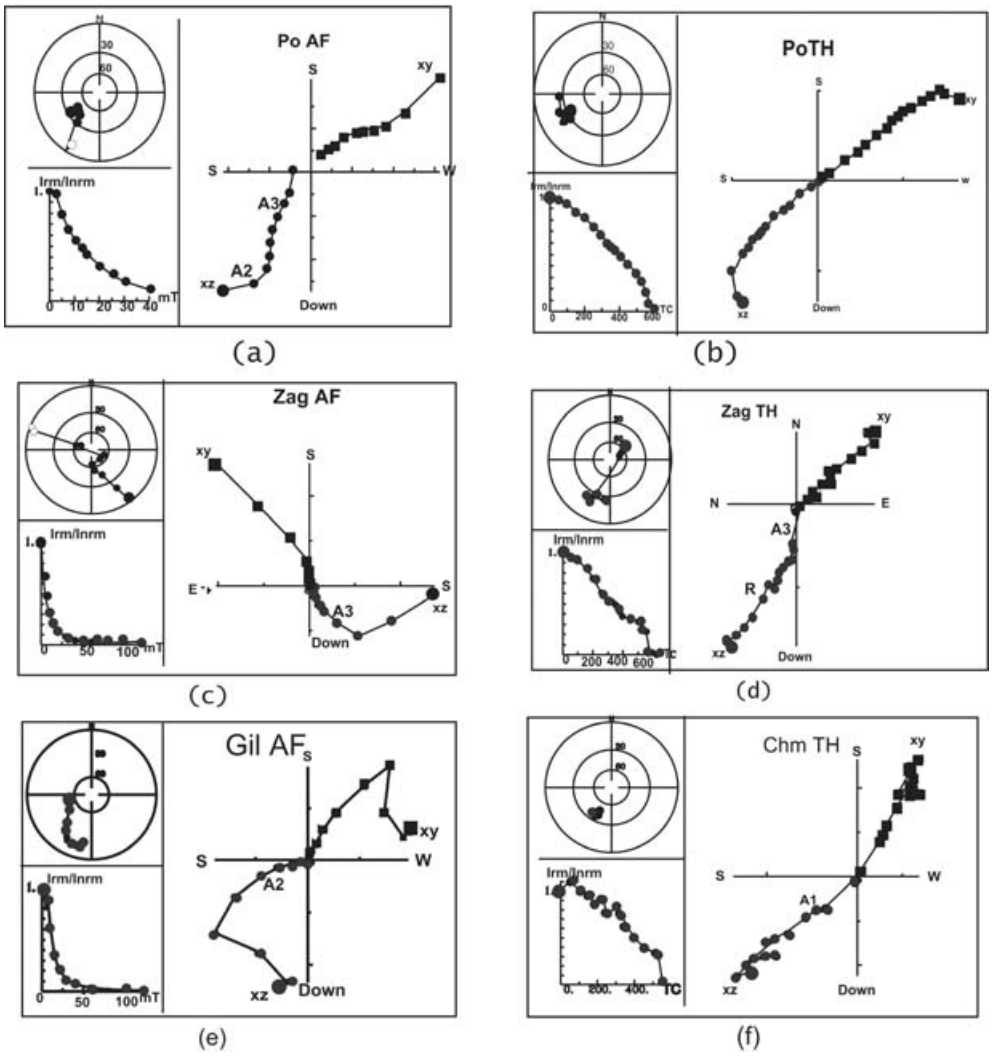

Figure 13. Examples of demagnetization results for specimens of GSB ultrabasic rocks (a) AF for Po (b) thermal for Po, (c) AF for Zag, (d) thermal for Zag, (e) thermal for Gil (f) thermal for Chm. Upper left-hand panel: stereographic projections of the NRM directions, full circles—positive inclinations, open circles—negative inclinations. Lower left-hand panel: decay of the intensity of NRM during step-like cleaning. Irm—intensity of NRM after consecutive cleaning steps, Inrm—intensity of the NRM before cleaning. Right—Zijderveld orthogonal projections in two planes: xz—full circles, xy—full squares.

demagnetized with TH and two with AF. The AF demagnetization results show low MDF (2.5–7 mT). The TH demagnetization curves reveal usually two components of NRM. One of them has either N or NW declination and intermediate–high inclination and is isolated in a broad range of unblocking temperatures, from 200°C to 550°C labelled R. It is often accompanied with another component isolated usually in temperature ranges beginning at about 450°C and ending at 600°C with SE or SW declinations and low–intermediate inclinations labelled A3 because of its similarity to the A3 components found in Ta and Jo. In some specimens it was found as a Hoffman-Day direction or a point of crossing of Halls great demagnetization circles. An example of demagnetizing result is shown in Figs 14(g) and (h), the stereographic projection of isolated directions—in Fig. 15(h).

6 DISCUSSION

Mineralogical and petrological investigations indicate that in each studied unit magnetite is the main magnetic mineral appearing in three generations formed due to consecutive pulses of serpentinization: alterations of olivines, pyroxenes, chromites and pyrrhotites. The oldest one (the 'flame chlorite' in Fig. 3) was present in Po and Zag. It could acquire magnetic remanence at the time of emplacement of ultrabasic xenoliths into GSB gneisses dated at 385–400 Ma, when the temperature attained about 600°C (Bylina *et al.* 2001). In Ta dunites from the JGSM there are small magnetite inclusions in olivine (Fig. 7b) that probably precede serpentinization episodes and could acquire thermal remanence when passing through temperatures corresponding to Tb's of magnetite. In JGSM serpentinites the oldest generation of magnetite is genetically related to oceanic serpentinization dated at *ca.* 400 Ma (Dubińska *et al.* 2004) and probably acquired remanence of chemical origin at that time. The consecutive magnetite generations as well as maghemite and haematite (martite) occurring in the studied rocks were formed later, probably during various tectonometamorphic events: (1) during continental recrystallization of serpentinite; (2) during uplift of the GSB (370–360 Ma, Gordon *et al.* 2005); (3) during the formation of the Niemcza Fault Zone (ca 340 Ma, Oliver *et al.* 1993); (4) during volcanic activity in the West Sudetes (Upper Permian); (5) during Tertiary rejuvenation of Sudetic fault; and (6) during recent weathering.

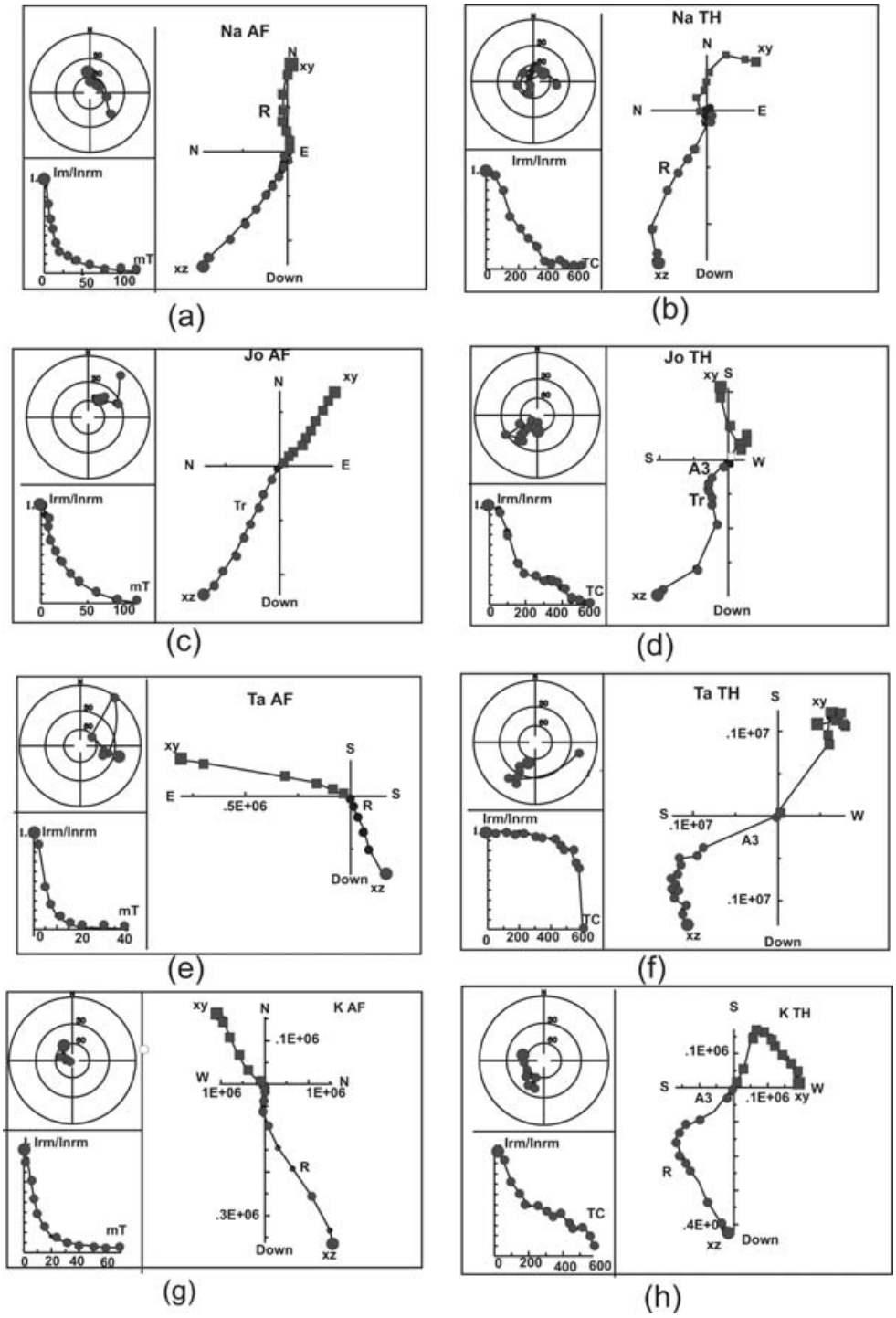

Figure 14. Examples of demagnetization results for specimens of JGSM ultrabasic rocks (a) AF for Na (b) thermal for Na, (c) AF for Jo, (d) thermal for Jo, (e) AF for Ta (f) thermal for Ta, (g) AF for K (h) thermal for K. Other symbols as in Fig. 13.

The five isolated components of NRM: R, Tr, A1, A2 and A3 are carried mostly by magnetite accompanied with minor magnetic minerals reflect directions of geomagnetic field from the time of consecutive events. The large scatter of palaeomagnetic directions within respective clusters seen in Fig. 15 can be related mainly to the extended persistence of remagnetization processes, and to irregular distribution of magnetic minerals in the studied samples as documented by significant variations of Km and NRM values. It is not clear which magnetite generation is responsible for particular isolated components. Generally, the AF cleaning was more effective in the GSB rocks than the thermal treatment, the demagnetizing curves usually clearly shown presence of two components carried by magnetite grains of different coercivities. However, in the JGSM rocks the presence of two components of NRM was evidently better observed in the TH cleaning than in AF.

The mean directions of isolated components appropriate for particular localities, together with their α_{95} are shown in Fig. 16. Table 4 summarizes mean directions together with Fisherian parameters and

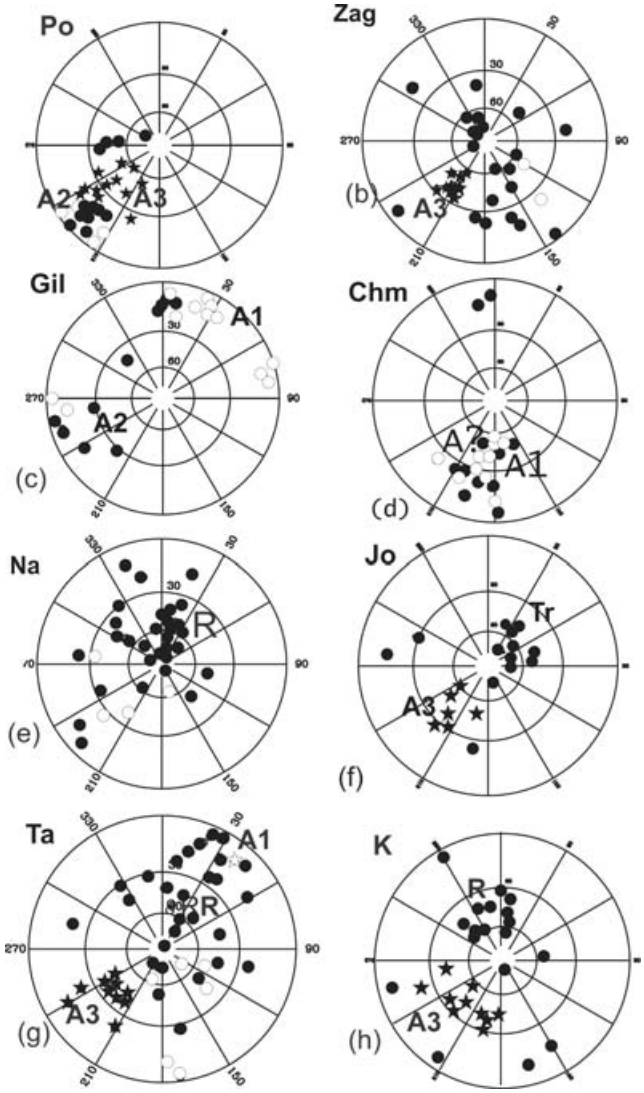

Figure 15. Stereographic projections of directions of the NRM components isolated due to AF and thermal demagnetization in each locality. (a–d)—results for GSB specimens (e–h)—results for JGSM specimens. Letters at the left side of each plot denote respective localities. R denotes group of Recent directions of components R, Tr—directions of component Tr, A1, A2 directions of components A1 and A2, stars denote directions of components A3, A?—directions of component A?. Full circles (stars)—positive inclinations, open circles (stars)—negative inclinations.

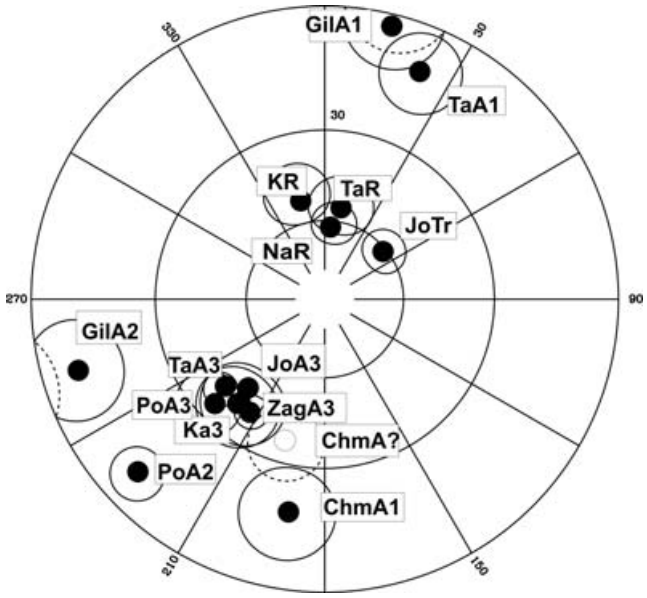

Figure 16. Stereographic plot of the mean directions of NRM isolated in GSB and JGSM units together with α_{95} confidence circles. Letters denote names of localities and respective components of NRM as in Fig. 15 and Table 4.

respective pole positions and palaeolatitudes. The pole positions are shown against the West Sudetic Apparent Polar Wander Path (Jeleńska *et al.* 2003) in Fig. 17.

The directions and pole positions of component R obtained for Na and Ta are consistent with the Tertiary-Recent reference data for the Stable Europe. (Besse & Courtillot 2002) The component R isolated in K is, perhaps, not fully isolated which makes the KR pole shifted from the NaR and TaR. The Tr component found in Jo yielded pole position fitting the reference data consistent with the reference Stable European data for the Late Triassic (Besse & Courtillot 2002).

The components A1 were isolated over the whole range of unblocking temperatures. Their directions and pole positions correspond to the Permo-Carboniferous segment of the Sudetic Path and are close to the primary magnetizations obtained for the Intra Sudetic Basin for the palaeontologically dated Stephanian-Autunian sediments (Kądziałko-Hofmokl & El-Hemaly 1997). They also fit the respective poles labelled A found in the gabbroic ophiolitic units Ślża and Nowa Ruda studied previously (Jeleńska *et al.* 1995). Closeness of the A components from Ślęża and Nowa Ruda, situated at different sides of the Sudetic Marginal Fault which cuts the GSB block, proves that there were no movements in this region at least since the Permo-Carboniferous times.

The component A2 was found only in the GSB. It is probably carried by coarse grains of magnetite and maghemite/haematite revealed by demagnetizing fields of about 40–50 mT and Tub's of 600°C–675°C. This component is probably of either chemical or thermochemical origin. The mean A2 direction and pole position obtained for the Po correspond to the palaeomagnetic results (pole position 13°S, 318°E) obtained for the palaeontologically dated Upper Devonian sediments from the Kłodzko Metamorphic Complex (Kądziałko-Hofmokl *et al.* 2003, and Table 4) and Bardo Basin (Jeleńska *et al.* 2001) and, by consequence, fits the Upper Devonian segment of the West Sudetic Path. This result indicates that the GSB massif was accreted to the West Sudetes during Upper Devonian. The direction and pole Gil A2 are significantly shifted from the Upper Devonian results. This shift may be explained as a result of movement and/or rotation of the Gil xenolith connected with the Niemcza Zone tectonic activity (e.g. Aleksandrowski *et al.* 2000). Rotation of the GilA2 pole around the Euler pole of 60°N, 20°E by 25° counter-clockwise (CCW) moves it to the vicinity of the PoA2 pole.

The most important is the overprint A3 observed in five localities, in 48 specimens cut from 22 individually oriented hand samples from both studied units. It was isolated by AF and TH cleaning as component of highest stability. We believe that it is of chemical origin in Po, Zag, Jo and K. In these localities this component is carried by fine grains of magnetite formed during the initial phase of serpentinization and was acquired when their volumes passed the critical values. In Ta component A3 may be of thermal and/or chemical origin. The common direction A3 calculated for five localities

Table 4. Palaeomagnetic results for the Gory Sowie Block and the Gogołów-Jordanów Serpentinite Massif.

Exposure	Component	N/n	D/I	α_{95}	k	Plat S	Plong E	Plat	*dp*/*dm*
Po	A2	16/5	227/8	6	42	22	325	4	3/6
	A3	12/5	228/35	10	21	8	332	20	7/11
Zag	A3	11/4	213/41	5.5	70	10	346	24	4/7
Gil	A1	11/3	14/2	10	23	39	358	1	5/10
	A2	10/5	254/8	11	19	7	302	4	6/11
	A2rot	10/5	224/8	14	19	24	327	4	6/11
Chm	A1	11/6	190/18	12	15	30	5	9	7/13
	A?	10/4	195/−37	11.5	18.5	58	349	21	8/13
Na	R	14/11	7/62	8	23	81	340	43	
Jo	Tr	11/5	51/62	8	32	55	278	44	10/13
	A3	6/3	218/43	13.5	25.3	7	343	25	10/17
Ta	R	14/6	10/56	11	13	74	325	37	12/16
	A1	13/5	23/11	9.5	20	41	345	6	5/10
	A3	9/4	229/40	5.5	87	6	334	23	4/7
K	R	11/6	345/51	11	20	68	53	31	10/14
	A3	10/6	219/41	13	15	8	341	24	10/16
GSB & JGSM	A3	5*	222/40	5.7	178	8	339	23	4/7
KMC (Kądziałko-Hofmokl *et al.* 2003)	Upper Devonian sediments	4*	237/16	16	33	13	318	8	9/17
FIC (Zwing & Bachtadse 2000)	363±7 Ma	20*	198/40	5	45	15	351	23	4/6

n/N—number of entries used for calculations/number of hand samples in which the respective component was isolated.
*—n the case of GSB & JGSM, KMC and FIC column 3 shows number of entries.
D/I—declination/inclination *in situ*, α_{95}, *k*—parameters of Fisherian statistics, PlatS—latitude of the southern palaeomagnetic pole position, SlatE—eastern longitude of the palaeomagnetic pole position, plat—palaeolatitude of the study area at the time of acquisition of respective remanence, *dp*/*dm*—half axes of the confidence ellipses.

Figure 17. Pole positions obtained in this paper together with their confidence ovals against the Apparent Polar Wander Path for the West Sudetes (Jeleńska *et al.* 2003). Numbers along the Path denote age in Ma.

and corresponding pole position are included in Table 4 and shown in Fig. 17. The A3 mean pole position lies significantly outside of the West Sudetic APWP, eastward of its oldest segment corresponding to the age of 394 Ma (Jeleńska *et al.* 2003). We therefore suppose that at that time the GSB & JGSM unit was not part of the West Sudetes.

Palaeolatitudes obtained for Ta, Jo. K and Zag sites range between 23°S and 25°S, palaeolatitude obtained for Po is 20°S and remains within the error limits of the other four. The declinations obtained for the five exposures range between 213° and 228° and also remain in the error limits. Unfortunately, it is not possible to perform any fold test for the studied units. However, the similarity of directions A3 obtained for five localities which represent different units suggest that they represent the overprint acquired at the same times in the same magnetizing field and that at those times both massifs formed one unit GSB & JGSM. The obtained palaeolatitudes agree with estimations of Tait *et al.* (2000) who situate the southern margin of Baltica at palaeolatitudes of 20°–30°S during the Late Silurian–Early Devonian (see Introduction) suggesting that the GSB & JGSM massif was situated close to the southern margin of Baltica during the Early Devonian.

Summarizing, we suppose that the A3 component was acquired between 380–400 Ma and that at that time the GSB and JGSM formed a unit situated close to the southern margin of Baltica. By the time of acquisition of the A2 component, dated by comparison with Late Devonian data obtained for palaeontologically dated sediments (Jeleńska *et al.* 2003; Kądziałko-Hofmokl *et al.* 2003), the unit was already accreted to the Sudetes. Thus the accretion probably took place by northward shift and rotation of the plate between 380 and 360 Ma.

The presented data support the idea of Devonian movements of individual blocks forming the ATA. One of the most reliable Devonian data for the ATA was obtained by Zwing & Bachtadse (2000) for the Frankenstein Intrusive Complex in the Mid-German Crystalline Rise dated at 363 ± 7 Ma (FIC in Table 4 and Fig. 17). The inclination (40°) indicates the Late Devonian palaeolatitude of this area as about 23°S. The FIC result implies its CCW rotation of about 27° against the Baltica plate after Middle Devonian, probably before Late Carboniferous—Permian.

Summing up, the data from FIC and data presented here agree with the idea of treating the ATA as a collage of numerous blocks (Tait *et al.* 2000) rotating against each other and against Baltica. It seems that the large units of ATA were composed of numerous smaller fragments, which moved northward and rotated before final accretion with Baltica.

The presented results do not contribute to the discussion of reliability of the Variscan orocline (Edel *et al.* 2003). However, our results reveal independent movements of small Sudetic units that took place in the Sudetic domain in the Early Devonian time. Comparison of the data obtained here with the Devonian data for FIC supports idea of movements of small blocks building the terranes of ATA before final accretion in Permo-Carboniferous times.

7 CONCLUSIONS

Petrological and palaeomagnetic study of the Sudetic ultrabasic rocks combined with their isotopic ages are promising source of information on the geotectonic position of major geological units of the Bohemian massif. The mineralogical and petrological study revealed that three generations of magnetite, including a partly oxidized phase (maghemite) from various JGSM and GSB ultrabasic rocks as well as Fe–Cr magnetic spinel from JGSM cumulate dunite, were main magnetic minerals in the studied rocks. Three groups of Palaeozoic palaeomagnetic directions as well as Triassic and recent palaeomagnetic components were found.

The results of the integrated palaeomagnetic and mineralogical study show that the GSB & JGSM plate was a separate unit of the accretionary prism during Early Devonian. GSB & JGSM plate palaeolatitude was stable during the period of 380–400 Ma and corresponded to the palaeolatitude of other units building the ATA and situated close to the southern margin of the Baltica plate. Taking into account the model of the West Sudetes APWP (Jeleńska *et al.* 2003) the authors assume that the GSB & JGSM plate shifted northward and rotated clockwise to the West Sudetes no earlier than 390 Ma.

ACKNOWLEDGMENTS

This research was founded by Institute of Geophysics, Polish Academy of Sciences (project 5/2003–2005) and by Institute of Geochemistry, Mineralogy and Petrology, Faculty of Geology, Warsaw University (projects: 1642/16 and 1642. The authors are indebted to Dr Piotr Dzierżanowski (Faculty of Geology, Warsaw University) for his assistance during microprobe studies, Mariusz Neska MSc, Anna Norberciak and Daniel Kuliński of the Institute of Geophysics, PAS for help in the field work and laboratory experiments.

REFERENCES

Aleksandrowski, P., Kryza, R., Mazur, S., Pin, C. & Zalasiewicz, J.A., 2000. The Polish Sudetes: Caledonian or Variscan, *Transactions of the Royal Society of Edinburgh,* **90,** 127–146.

Anonymous, 1972. Penrose Field Conference on Ophiolites, *Geotimes.,* 24–25.

Besse, J. & Courtillot, V., 2002. Apparent and true polar wander and the geometry of the geomagnetic field over the last 200 Myr, *J. geophys. Res.,* **107**(B11), doi:10.1029/2000JB000050.

Brueckner, H.K., Blusztajn, J. & Bakun-Czubarow, N., 1996. Trace element and Sm-Nd 'age' zoning in garnets from peridotites of the Caledonian and Variscan Mountains and their tectonic implications, *Journal of Metamorphic Geology,* **14**(1), 61–73.

Bylina, P., Dubińska, E., Kozłowski, A., Dörr, W., Nejbert, K. & Schastok, J., 2001. Glimmerite from Potoczek (Góry Sowie, SW Poland): Record of ultramafic body emplacement into migmatitic gneisses, *Mineralogical Society of Poland* - Special Papers, **19,** 30–32.

Cherniak, D.J. & Watson, E.B., 2000. Pb diffusion in zircon, *Chemical Geology,* **172,** 5–24.

Day, R., Fuller, M. & Schmidt, V.A., 1977. Hysteresis properties of titanomagnetites: Grain size and composition dependence, *Phys. Earth planet. Int.* **13,** 260–267.

Dubińska, E., 1995. Rodingites of the eastern part of Jordanów-Gogołów serpentinite massif, Lower Silesia, Poland, *Canadian Mineralogist,* **33,** 585–608.

Dubińska, E., Bylina, P., Kozłowski, A., Dörr, W., Nejbert, K., Schastock, J. & Kulicki, C., 2004. U-Pb dating of serpentinization: hydrothermal zircon from a metasomatic rodingite shell (Sudetic ophiolite, SW Poland), *Chemical Geology,* **203,** 183–203.

Dubińska, E. & Gunia, P., 1997. The Sudetic ophiolite: current view on its geodynamic model, *Geological Quarterly,* **41,** 1–20.

Dubińska, E., Żelaźniewicz, A., Nejbert, K. & Bylina, P., 1999. Ultramafic rocks from migmatitic gneisses of the Góry Sowie block, Sudetes, *Mineralogical Society of Poland—Special Papers,* **14,** 76–79.

Dubińska, E., Bylina, P. & Nejbert, K., 2002. Retrogression metamorphism of ultrabasic rocks from Góry Sowie Block and Sudetic Ophiolite, *Mineralogical Society of Poland—Special Papers,* **20,** 81–84.

Dunlop, D., 1974. Thermal enhancement of magnetic Susceptibility, *J. Geophys.,* **40,** 439–451.

Dunlop, D.J., 2002. Theory and application of the Day plot (Mrs/Ms vs Hcr/Hc):2. Application to data for rocks, sediments and soils, *J. geophys. Res.,* **107**(B3), EPM 4-1–EPM 4-2.

Dunlop, D.J. & Özdemir, Ö., 1996. *Rock magnetism,* Cambridge Univ. Press. Cambridge, 573 pp

Edel, J.B., Schulman, K. & Holub, F.V., 2003. Anticlockwise and closcwise rotations of Eastern Variscides accomodated by dextral lithospheric wrenching: paleomagnetic and structural evidence. 2003, *J. geol. Soc. Lond.,* **160,** 209–218.

Fernandes, T.R.C., 1999. Significance and ferrimagnetism in chromitites from the Great Dyke, Zimbabwe, *Journal of African Sci.,* **28**(2), 337–348.

Franke, W. & Żelaźniewicz, A., 2000. Structure and evolution of the Bohemia, in *Paleozoic Amalgamation of Central Europe,* Vol. 201, pp. 279–293, eds Wimchester, J.A., Pharaoh, T.C. & Verniers, J., Geological Society, London, Special Publications.

Frost, B.R., 1985. On the stability of sulfides, oxides, and native metals in serpentinite, *J. Petrol.,* **26,** 31–63.

Gapeev, A.K., Gribov, S.K., Dunlop, D.J., Özdemir Ö. & Shcherbakov, V.P., 1991. A direct comparison of the properties of CRM and VRM in the low temperature oxidation of magnetite, *Geophys. J. Int.,* **105,** 407–418.

Gordon, S.M., Schneider, D.A., Manecki, M. & Holm, D.K., 2005. Exhumation and metamorphism of an ultrahigh-grade terrane; geochronometric investigations of the Sudete Mountains (Bohemia), Poland and Czech Republic, *J. geol. Soc. Lond.,* **162,** 841–855.

Grove, M. & Harrison, T.M., 1996. $^{40}Ar^{*}$ diffusion in Fe-rich biotite, *American Mineralogist,* **81,** 940–951.

Gunia, P., 1997. Petrology of ultrabasic rocks from the Góry Sowie block, *Prace Geologiczno-Mineralogiczne,* **LXV,** 1–78 (in Polish).

Halls, H.C., 1976. A least-squares method to find a remanence directionfrom converging remagnetization circles, *Geophys. J. R. astr. Soc.,* **45.** 297–304.

Hames, W.E. & Bowring, S.A., 1994. An empirical evaluation of argon diffusion geometry in muscovite, *Earth planet. Sci. Lett.,* **124,** 161–167.

Harrison, T.M., 1981. Diffusion of ^{40}Ar in hornblende, *Contribution to Mineralogy and Petrology,* **78,** 324–331.

Jamrozik, L., 1989. Strefa mineralizacji ilmenitowej Strzegomiany-Kunów w intruzji gabrowej Ślęży w obrębie ofiolitu Sobótki (Dolny Śląsk). *Przegląd Geologiczny,* **37**(10), 477–485 (Strzegomiany-Kunów zone enriched in ilmenite within the gabbroic Ślęża intrusion, Lower Silesia, in Polish with English summary).

Jeleńska, M., Aifa, T., Kądziałko-Hofmokl, M. & Żelaźniewicz, A., 2001. Paleomagnetic and rock-magnetic study of Devonian olistholits in Early Carboniferous flysh, West Sudetes, Poland, *Geophys. J. Int.,* **122,** 658–674.

Jeleńska, M., Kądziałko-Hofmokl, M. & Żelaźniewicz, A., 2003. The Devonian—Permian APWP for the West Sudetes, Poland, *Stud. Heophys. Geod.,* **47,** 419–434.

Jeleńska, M., Kądziałko-Hofmokl, M., Edel, J.B., Jamrozik, L., Petersen, N. & Soffel, H., 1995. Paleomagnetic investigations of the Paleozoic circum-Sowie Góry Mts ophiolitic belt in the Sudetes, *Geophys. J. Int.,* **122,** 658–674.

Kądziałko-Hofmokl, M., 2001. Rock-magnetic study of the Gogołów-Jordanów serpentinite unit of the Paleozoic Sudetic ophiolite (South Poland), *Ofioliti.* **26**(2b), 425–432.

Kądziałko-Hofmokl, M. & El-Hemaly, I., 1997. Paleomagnetism of Carboniferous sediments from the West Sudetes (SW Poland), *Geologie en Mijnbouw,* **76,** 97–104.

Kądziałko-Hofmokl, M. & Kruczyk, J., 1976. Complete and partial self-reversal of natural remanent magnetization in basaltic rocks from Lower Silesia, *Pageoph,* **114,** 207–213.

Kądziałko-Hofmokl, M., Kruczyk, J., Mazur, S. & Siemiątkowski, J., 2003. Paleomagnetism of Upper Proterozoic and Devonian rocks from the Kłodzko Metamorphic Complex in the West Sudetes (SW Poland): tectonic implications for the Variscan belt of Central Europe, *Tectonophysics,* **377,** 83–99.

Kirschvink, J.L., 1980. The least squares line and plane analysis of paleomagnetic data, *Geophys. J. R. astr. Soc.,* **62,** 699–718.

Kröner, A. & Hegner, E., 1998. Geochemistry, single zircon ages and Sm-Nd systematics of granitoid rocks from the Góry Sowie (Owl Mts), Polish West Sudetes: evidence for early Paleozoic arc-related plutonism. *J. Geol. Soc.,* **155**(4), 711–724.

Leake, B.E. *et al.*, 1997. Nomenclature of amphiboles: Report of the Subcommittee on Amphiboles of the International Mineralogical Association on New Minerals and Names, *American Mineralogist,* **82,** 1019–1037.

Lewandowski, M., Werner, T. & Nowożyński, K., 1997. PDA—a program package of Fortran programs for paleomagnetic data analysis, *Inst. Geophys. Pol. Ac. Sci. Manuscript,* 1–17.

Liou, J.G., Zhang, R.Y., Ernst, W.G., Rumble, D. III. & Maruyama, S., 1998. High-pressure minerals from deeply subducted metamorphic rocks, in *Ultrahigh-Pressure Mineralogy: Physics and Chemistry of the Earth Deep Interior,* Vol. 37, pp. 33–96, ed. Hemley, R.J., Reviews in Mineralogy, Mineralogical Society of America, Washington, DC.

Majerowicz, A., 1979. The Mountain Group of Ślęża and recent petrological problems of the ophiolites, Selected Stratigraphical, Petrographical and Tectonic Problems of the Eastern Border of the gneisses of Sowie Góry Mts. and Kłodzko Metamorphic Structure, in *Materiały Konferencji Terenowej, Nowa Ruda,* Wydawnictwo Uniwersytetu Wrocławskiego, 9–34 (in Polish).

Marheine, D., Kachlik, V., Maluski, H., Patočka, F. & Żelaźniewicz, A., 2002. The ^{40}Ar–^{39}Ar ages from the West Sudetes (NE Bohemian massif): constraints on the Variscan polyphase tectonothermal development. In: Winchester, J., Pharaoh, T. & Verniers, J. (eds), Paleozoic Amalgamation of Central Europe, Special Publication, *Geological Soc. of London,* **201,** 133–135.

McFadden, P.L. & McElhinny, M.W., 1988. The combined analysis of remagnetization circles and direct observation in paleomagnetism, *Earth planet. Sci. Lett.,* **87,** 161–172.

Mezger, K., Essene, E.J. & Halliday, A.N., 1992. Closure temperatures of the Sm-Nd system in metamorphic garnets, *Earth planet. Sci. Lett.,* **113,** 397–409.

Morris, A., 2003. A paleomagnetic and rock magnetic glossary. *Tectonophysics,* **377**(1–2), 211–228.

O'Brien, P.J., Kröner, A., Jaeckel, P., Hegner, E. & Żelaźniewicz, A., 1997. Petrological and isotopic studies on Paleozoic high pressure granulites with a medium pressure overprint, Gory Sowie mts. Polish Sudetes, *J. Petrol.,* **38,** 433–456.

Oliver, G.J.H., Corfu, F. & Krogh, T.E., 1993. U-Pb ages from SW Poland: evidence for a Caledonian suture zone between Baltica and Gondwana, *Journal of Geological Society,* London, v. **150,** 355–369.

Orlicky, O., 1990. Detection of magnetic carriers in rocks: results of susceptibility changes in powdered rock samples induced by temperature, *Phys. Earth planet. Int.,* **63,** 66–70.

Orlicky, O., 1994. Study and detection of magnetic minerals by means of the measurement of their low-field susceptibility changes induced by temperature, *Geologica Carpathica,* **45**(2), 113–119.

Peters, C. & Dekkers, M.J., 2003. Selected room temperature magnetic parameters as function of mineralogy, concentration and grain size, *Physics and Chemistry of the Earth.,* **28,** 659–667.

Porębski, S.J., 1990. Onset of coarse clastic sedimentation in the Variscan realm of the Sudetes (SW Poland): An example from the Upper Devonian-Lower Carboniferous Świebodzice succesion, *Neues Jahrbuch fr Geloogie und Palaeontologie Abhandlungen,* **179,** 259–274.

Schmidbauer, E., 1969. Magnetic properties of oxidized Fe-Cr spinels. *Zeitschrift für Geophysik. B.,* **35,** 475–484.

Schmidbauer, E., 1971. Magnetization of Fe-Cr spinels and its application for identification of such ferrites in rocks, *Zeitschrift für Geophysik. B.* **37,** 421–424.

Tait, J., 1999. New Early Devonian paleomagnetic data from NW France: Paleogeography and implications for the Armorican microplate hypothesis, *J. geophys. Res.,* **104**(B2), 2831–2839.

Tait, J., Schätz, M., Bachtadse, V. & Soffel, H., 2000. Paleomagnetism and Paleozic paleogegraphy of Gondwana and European terranes, in *Orogenic Processes: Quantification and Modelling in the Variscan Belt,* Vol. 179, pp. 21–34, eds Franke, W., Hakk, V., Oncken, O. & Tanner, D., Geol. Soc. London, Special Publications.

Torsvik, T. & Smethurst, M.A., 1994. GMAP for Windows (V.1)—Geographic Mapping and Paleoreconstruction Package (*Manual*). NGU Trondheim, Norway

van Breemen, O., Bowes, D.R., Aftalion, M. & Żelaźniewicz, A., 1988. Devonian tectonothermal activity in the Góry Sowie gneissitic block, Sudetes, SW Poland: evidence from Rb-Sr and U-Pb isotopic studies, *Annales Societatis Geologorum Poloniae,* **58,** 3–19.

van Welzen, A., 1992. The influence of weathering on the magnetic properties of single domain magnetite in marine sediments, *Geol Ultraiectina,* **122**. 45–65.

Winchester, J.A. & The PACE TMR Network Team. 2002. Palaeozoic amalgamation of Central Europe: new results from recent geological and geophysical investigations, *Tectonophysics,* **360,** 5–21.

Yu, Y., Dunlop, D.J., Özdemir Ö. & Ueno, H., 2001. Magnetic properties of Kurokami pumices from Mt. Sakurajima, Japan, *Earth planet. Sci. Lett.,* **192,** 439–446.

Zahniser, S. J., 2004. Tectonometamorphic evolution of an allochtonous terrane, Góry Sowie Block, northeastern Bohemian massif (Poland). *MSc. Thesis,* College of Arts and Sciences, Ohio University, 76pp.

Zwing, A. & Bachtadse, V., 2000. Paleoposition of the northern margin of Armorica in Late Devonian times; Paleomagnetic and rock magnetic results from the Frankenstein Instrusive Complex (Mid-German Crystalline Rise), *J. geophys. Res.,* **105**(89), 21 445–21 456.